KTH Engineering Sciences

Analytical and Numerical Analysis of the Acoustics of Shallow Flow Reversal Chambers

Supervisor:

Mats Åbom

Student:

Alireza Qazizadeh

Master of Science Thesis in Technical Acoustics
Stockholm, Sweden
March, 2012
TRITA-AVE 2012:16

1 Contents

2 Introduction

Flow reversal chambers are mainly used to accomplish a compact silencer design needed on a vehicle. Generally in this configuration the inlet and outlet ports are on the same face and the flow direction is reversed.

During many years different authors have tried to develop 1D and 3D models for evaluating the acoustic performance of circular and rectangular reversing chambers.

Ih [1] categorizes four methods for evaluating the acoustic performance of the reversing chamber. The first involves utilizing analysis techniques for other types of muffler elements having similar acoustic performances [2]. Analysis techniques for extended inlet/outlet expansion chambers may be used to approximate the behavior of a reversing chamber in which the length-to-diameter ratio is large. When the length-to-diameter ratio is small, the reversing chamber approximates the behavior of a short expansion chamber. In this case, exact predictions of the acoustic performances cannot be made and, moreover, the method itself is a trial-and-error one. The second is a mode-matching method at the discontinuities [3-5], but this is tedious to formulate and the transmission matrix for this type of muffler has not been obtained. A simplified version (third method) of this method has been developed for plane wave propagation, in which the sound pressures and particle velocities at the area discontinuities are matched [6, 7]. However, this method is restricted to a very small frequency range below the cut-off frequency of the first asymmetric mode, i.e., the (1, 0) mode, and the peaks of the transmission loss curves are not correctly predicted due to the disregard of the higher order modes. Furthermore, when the length-to-diameter ratio is small, the actual acoustic performance deviates appreciably from the theoretical transmission loss predicted by this one-dimensional analysis method. The fourth method involves using numerical methods such as finite element analysis [8] and the finite difference method [9], or possibly, the boundary element method. These numerical techniques have some merits in the treatment of more complicated geometries, such as that of an elliptic cross-section and/or a chamber with a pass tube [10], but a great many mesh points or mesh elements are required to deal with the high frequency range, so that the execution time for computation is long and the costs are high. It is also difficult to describe the total exhaust system by incorporating the transmission matrix of each silencer element.

Lindborg et al. [11] modeled the flow reversal chamber by two port method. The system under study is broken down into a set of linear subcomponents that are described individually and then assembled in a network. Each component is treated as a black box that is defined at the inlet and outlet ports where plane waves are assumed. This is an efficient tool, but for complicated geometries such as the flow reversal chamber the decomposition into subcomponents is not obvious.

Three different approaches are used for the two port modeling of a flow reversal [11];
1- Large quarter wave resonator
2- More detailed representation consisting of cones and quarter wave resonators
3- A simplification of the second approach into a simple Pipe

From the results of this study, it can be concluded that the acoustic characteristics of shallow flow reversal chambers can be modeled, with engineering precision, up to cut on frequency of the first higher order mode using simple two-port elements. Good results were achieved modeling the flow reversal chamber as a simple straight duct connecting the inlet and the outlet.

Munjal [12] devised a numerical collocation method. This method is easily applicable to rectangular as well as circular expansion chambers, but is limited to integer multiple area expansion ratios due to its inherent concept of discrete geometrical partitioning.

Analytical methods have been introduced over the years. These methods fall into two main groups, one-dimensional and three-dimensional models. However as Ih [13] has mentioned, if the length of the chamber is much shorter than its width, then a large number of modes should be counted for calculating transmission loss even for the very low frequency range and this fact, arising mainly from the higher order acoustic modes generated at area discontinuities which do not fully decay before they reach the counterpart port, because the inlet and outlet are very close to each other. This leakage phenomenon means that the one-dimensional models are quite far from the actual performances even in the low frequency region.

Three-dimensional models provide a very simple and exact approach to theoretical prediction of acoustical performance of plenum and reversing chambers. A three-dimensional mathematical formulation for mufflers with circular or rectangular cross-section with arbitrary location of inlet/outlet is derived by using the Eigen function expansion technique by Ih [13, 14]. The same problem is solved by the use of Green's function by Kim and Kang [15] for circular chambers and by Venkatesham et al. [16] for rectangular chambers. These methods take into account the effect of higher order modes which is necessary for successful analysis of a flow reversal chamber. The basic idea for these models stems from the fact that these chambers are in general regular in shape, which permits the use of series of orthogonal eigenfunctions.

However, mufflers used in industry are not exactly rectangles or cylinders. Usually they are a bit curved at the edges to increase the stiffness. It is of interest for industry to know how this difference can alter the TL curve. This problem can be solved by FEM, however this method would be expensive and time consuming. One purpose of this thesis work is to investigate other methods for predicting TL of such chambers.

One method could be to approximate the chamber which is curved at the edges with one which has sharp edges and then use the available theoretical models like the Green's function method to get TL curve. In the present study we want to find out how to do this approximation. The other possible method can be Neural Network. However this method needs some training data to train the neural network. Data for training can be obtained either through experiment or FEM.

The effect of mean flow velocity is not studied here; However it has been found to be of negligible effect when Mach number is smaller than about 0.03 [17]. Besides, when the mean flow velocity is smaller than about M = 0.1, the convective contributions can be considered as negligible second order quantities and flow-generated noise may often be neglected. Further, if the mean flow velocity is small, the flow-generated

noise as well as pressure losses can be greatly reduced without degradation of the acoustic performance by streamline guidance: i.e., by using special l/O connecting geometries such as bell mouths and perforated bridges with high perforation ratios over 20% [14].

3 Theoretical formulation

In this part three analytical methods for calculating Transmission Matrix (TM) and Transmission Loss (TL) of flow reversing chambers are presented where the two first ones are for rectangular chambers and the last one is for cylindrical chambers. However, first TM and TL are defined as follows,

TM connects the acoustic pressure and volume velocity in the inlet to the same state variables in the outlet and can be defined as:

$$\begin{bmatrix} \bar{p}_1 \\ v_1, U_1 \end{bmatrix} = \begin{bmatrix} T_{11} & T_{12} \\ T_{21} & T_{22} \end{bmatrix} \begin{bmatrix} \bar{p}_2 \\ v_2, U_2 \end{bmatrix} \tag{3-1}$$

Where
$\bar{p}$: Complex pressure at inlet or outlet
v or U : Complex volume velocity at inlet or outlet
$TM = \begin{bmatrix} T_{11} & T_{12} \\ T_{21} & T_{22} \end{bmatrix}$: Transmission matrix (The four elements of the TM are called four-pole parameters)

Once TM is found, transmission loss (TL) can be expressed in terms of the four pole-parameters as [19].

$$TL = 20\log_{10}\left\{\left(Z_2 / Z_1\right)^{1/2}\left|T_{11} + T_{12}/Z_2 + T_{21}Z_1 + T_{22}\left(Z_1 / Z_2\right)\right| / 2\right\} \qquad dB \tag{3-2}$$

where Z_1 and Z_2 are characteristic impedances of the inlet duct and outlet duct, respectively: $Z_1 = \rho_0 c_0 / S_1$ and $Z_2 = \rho_0 c_0 / S_2$, where $S_1 = a_1 b_1$ and $S_2 = a_2 b_2$ are areas of each corresponding port, here assumed rectangular. The linearity of the system can be assured by checking the reciprocity relation of $T_{11}T_{22} - T_{12}T_{21} = 1$.

The first analytical method that will be discussed here, suggested by B. Venkatesham et al. [16], is based on the Green's function of a rectangular cavity with homogeneous boundary conditions. The rectangular chamber Green's function is expressed in terms of a finite number of rigid rectangular cavity mode shapes. The second and third methods, suggested by Ih [13, 1], are derived by using eigenfunction expansion technique. These methods are discussed in parts 3.1 to 3.3.

The Green's function method has an advantage in modeling the absorptive boundary conditions and also flexible walls. Comparing the first and second methods, it was found that it's easier to follow the theoretical formulation of the first method and it is also easier to code it in MATLAB.

3.1 Green's function method

3.1.1 Green's function derivation

Figure 1shows the schematic diagram of a simple rectangular reverse flow expansion chamber. If the dimensions of the inlet and outlet port were small compared to wavelength, then the uniform velocity assumption would be valid. Green's function for rectangular cavity in terms of the cavity mode shapes is given by [20]

$$G(\vec{x} \mid \vec{x}_0) = \sum_{mpn} \frac{\overline{\psi}_{mpn}(\vec{x})\psi_{mpn}(\vec{x}_0)}{k^2{}_{mpn} - k^2} \tag{3-3}$$

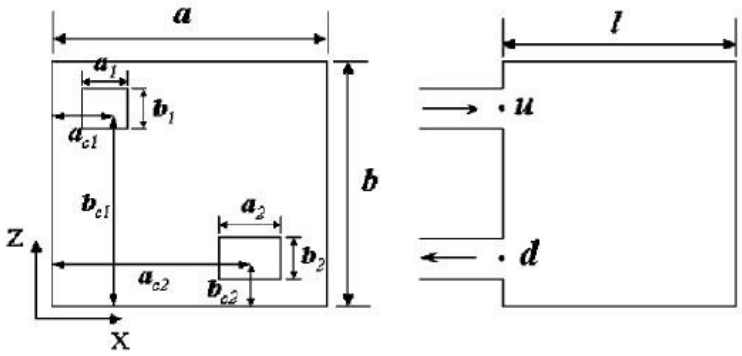

Figure 1 Schematic diagram of a rectangular reverse flow expansion

Here,

$k = \omega / c_0$ is the wavenumber, and the mode shape of a rectangular cavity is given by [20]

$$\psi_{mpn}(\vec{x}) = \cos\frac{m\pi x}{a}\cos\frac{p\pi y}{l}\cos\frac{n\pi z}{b} \tag{3-4}$$

with the corresponding wavenumber and the natural frequency as

$$k_{mpn} = \left[\left(\frac{m\pi}{a}\right)^2 + \left(\frac{p\pi}{l}\right)^2 + \left(\frac{n\pi}{b}\right)^2\right]^{1/2} \tag{3-5}$$

and

$$\omega_{mpn} = \pi c_0\left[\left(\frac{m}{a}\right)^2 + \left(\frac{p}{l}\right)^2 + \left(\frac{n}{b}\right)^2\right]^{1/2} \tag{3-6}$$

and the orthonormal function $\overline{\psi}_{mpn}(\vec{x})$ is written as

$$\overline{\psi}_{mpn}(\vec{x}) = \frac{e_m e_p e_n}{V}\psi_{mpn}(\vec{x}) \tag{3-7}$$

Here, $\vec{x}$ and $\vec{x}_0$ are the response coordinates vector and source coordinates vector, respectively; n, p and m are integers; a, l and b are dimensions (in m) of the rectangular expansion chamber in the x, y and z coordinate directions, as shown in Figure 1; and V is volume of the chamber ($V = alb$). The normalization factors are given by:

$$\begin{aligned} e_m &= \begin{cases} 1 & for\ m = 0 \\ 2 & for\ m \geq 1 \end{cases} \\ e_n &= \begin{cases} 1 & for\ n = 0 \\ 2 & for\ n \geq 1 \end{cases} \\ e_p &= \begin{cases} 1 & for\ p = 0 \\ 2 & for\ p \geq 1 \end{cases} \end{aligned} \tag{3-8}$$

and c_0 is speed of sound in m/s. Substituting Eq. (3-7) into Eq. (3-3) yields

$$G(\vec{x} \mid \vec{x}_0) = \sum_{mpn} \frac{e_m e_p e_n}{V} \frac{\psi_{mpn}(\vec{x}) \psi_{mpn}(\vec{x}_0)}{k^2{}_{mpn} - k^2} \tag{3-9}$$

The acoustic wave equation that determines the acoustic field in the rectangular chamber can be expressed as [20]

$$\nabla^2 \phi + k^2 \phi = -Q(\vec{x}) \tag{3-10}$$

where Q is the embedded source, if any, for the sake of generality.

Assuming harmonic time behavior, the velocity potential may be written as $\phi(\vec{x}, t) = \phi(\vec{x}) e^{j\omega t}$. Thus, acoustic pressure

$$p(\vec{x}, t) = -\rho \frac{\partial \phi(\vec{x}, t)}{\partial t} = -\rho j \omega \phi(\vec{x}) \tag{3-11}$$

and particle velocity

$$u(\vec{x}) = grad\ \phi(\vec{x}) = \nabla \phi(\vec{x}) \tag{3-12}$$

3.1.2 Derivation of the velocity potential

Total velocity potential inside the chamber is expressed by superimposing the velocity potentials generated due to the inlet and outlet piston sources. Thus, the expression for total velocity potential can be written as [15]

$$\phi(\vec{x}) = -\left[\int \int G(\vec{x} \mid \vec{x}_0) N_1(x_0, z_0) ds_A + \int \int G(\vec{x} \mid \vec{x}_0) N_2(x_0, z_0) ds_A \right] \tag{3-13}$$

Let us assume

$$\phi_1(\vec{x}) = -\int\int_{piston1} G(\vec{x} \mid \vec{x}_0) N_1(x_0, z_0) dxdz \tag{3-14}$$

and

$$\phi_2(\vec{x}) = -\int\int_{piston2} G(\vec{x} \mid \vec{x}_0) N_2(x_0, z_0) dxdz \tag{3-15}$$

where

$$\begin{aligned} N_1(x_0, z_0) = u_1 &\left[H\left\{ x - \left(a_{c1} - \frac{a_1}{2} \right) \right\} - H\left\{ x - \left(a_{c1} + \frac{a_1}{2} \right) \right\} \right] \\ &\left[H\left\{ z - \left(b_{c1} - \frac{b_1}{2} \right) \right\} - H\left\{ z - \left(b_{c1} + \frac{b_1}{2} \right) \right\} \right] \equiv u_1 f_1(x_0, z_0) \end{aligned} \tag{3-16}$$

$$\begin{aligned} N_2(x_0, z_0) = u_2 &\left[H\left\{ x - \left(a_{c2} - \frac{a_2}{2} \right) \right\} - H\left\{ x - \left(a_{c2} + \frac{a_2}{2} \right) \right\} \right] \\ &\left[H\left\{ z - \left(b_{c2} - \frac{b_2}{2} \right) \right\} - H\left\{ z - \left(b_{c2} + \frac{b_2}{2} \right) \right\} \right] \equiv u_2 f_2(x_0, z_0) \end{aligned} \tag{3-17}$$

Here, H is Heaviside function, and u_1 and u_2 are velocities of the hypothetical pistons at the inlet and outlet, respectively. Substituting the Green's function expression (3-9) into Eq. (3-14) gives

$$\begin{aligned} &\phi_1(x, y, z) = \\ &-\int_{b_{c1}-\frac{b_1}{2}}^{b_{c1}+\frac{b_1}{2}} \int_{a_{c1}-\frac{a_1}{2}}^{a_{c1}+\frac{a_1}{2}} \sum_{mpn} \frac{e_m e_p e_n}{V} \frac{\psi_{mpn}(x, y, z)}{k^2{}_{mpn} - k^2} \psi_{mpn}(x_0, y_0, z_0) u_1 \; f_1(x_0, z_0) dx_0 dz_0 \end{aligned} \tag{3-18}$$

$$= u_1 \sum_{mpn} \frac{e_m e_p e_n}{V} \frac{\psi_{mpn}(\vec{x})}{k^2{}_{mpn} - k^2} \left[\cos\frac{p\pi y_0}{l} C_{m1} C_{n1} \right] \tag{3-19}$$

where

$$C_{m1} = \begin{cases} a_1 & for\ m = 0 \\ \dfrac{2a}{m\pi} \cos\left(\dfrac{m\pi a_{c1}}{a} \right) \sin\left(\dfrac{m\pi a_1}{2a} \right) & for\ m \neq 0 \end{cases} \tag{3-20}$$

and

$$C_{n1}=\begin{cases} b_1 & for\ n=0 \\ \dfrac{2b}{n\pi}\cos\left(\dfrac{n\pi b_{c1}}{b}\right)\sin\left(\dfrac{n\pi b_1}{2b}\right) & for\ n\neq 0 \end{cases} \tag{3-21}$$

Similarly, velocity potential ϕ_2 due to the piston source at the outlet maybe obtained. Generalizing the results, the velocity potential caused by port *i* can be written as

$$\phi_i(\vec{x})=\sum_{mpn} S^i_{mpn}\psi_{mpn}(\vec{x}) \tag{3-22}$$

where

$$S^i_{mpn}=\frac{(-1)^i e_m e_p e_n \cos(p\pi y_{io}/l)}{k^2_{mpn}-k^2}\frac{C_{mi}C_{ni}u_i}{V} \tag{3-23}$$

and ψ_{mpn} is given by Eq. (3-4), and C_{mi}, C_{ni} are given by Eqs. (3-20) and (3-21), with subscript 1 being replaced by i; where $i=$ 1 and 2.

3.1.3 The transfer matrix derivation

The transmission loss of the chamber, which expresses the performance of the rectangular chamber, can be obtained from the four-pole parameters, which in turn maybe derived from the velocity potentials. Making use of Eq. (3-11), acoustic pressure is written as $p_i=-j\omega\rho_0\phi_i(\vec{x})$.

The average sound pressure acting on the piston ‘‘*i*’’ with cross-sectional area ‘‘ A_i ’’ by the velocity field, which is generated by the rectangular piston ‘‘*i*’’, can be written as

$$\bar{p}_{ii'}=-\frac{j\omega\rho_0}{A_i}\iint_{piston\ i}\phi_{i'}(\vec{x})ds_i \tag{3-24}$$

or

$$\bar{p}_{ii'}=-\frac{j\omega\rho_0}{A_i}\int_{b_{ci}-\frac{b_i}{2}}^{b_{ci}+\frac{b_i}{2}}\int_{a_{ci}-\frac{a_i}{2}}^{a_{ci}+\frac{a_i}{2}}\phi_{i'}dzdx \tag{3-25}$$

Substituting Eq. (3-22) into Eq. (3-25) gives

$$\bar{p}_{ii'}=-\frac{j\omega\rho_0}{A_i}\int_{b_{ci}-\frac{b_i}{2}}^{b_{ci}+\frac{b_i}{2}}\int_{a_{ci}-\frac{a_i}{2}}^{a_{ci}+\frac{a_i}{2}}\left(\sum_{mpn}S^{i'}_{mpn}\psi_{mpn}(\vec{x})dzdx\right) \tag{3-26}$$

Substituting Eq. (3-23) into Eq. (3-26) gives

$$\bar{p}_{ii'} = (-1)^{i'} \frac{j\omega\rho_0 u_{i'}}{A_i} \sum_{mpn} \frac{e_m e_p e_n}{V} \frac{(-1)}{k_{mpn}^2 - k^2} \times \cos\left(\frac{p\pi y_{i'o}}{l}\right) \cos\left(\frac{p\pi y_{io}}{l}\right) C_{mi'} C_{ni'} C_{mi} C_{ni} \tag{3-27}$$

By rearranging the terms, it can be expressed as

$$\bar{p}_{ii'} = \frac{(-1)^{i'}}{A_i A_{i'}} jZ_0 v_{i'} \sum_{mpn} \frac{e_m e_p e_n}{l} \left(\frac{-k}{k_{mpn}^2 - k^2}\right) \times \cos\left(\frac{p\pi y_{i'o}}{l}\right) \cos\left(\frac{p\pi y_{io}}{l}\right) C_{mi'} C_{ni'} C_{mi} C_{ni} \tag{3-28}$$

Here, $Z_0 = \rho_0 c_0 / S$ is the characteristic impedance of the chamber, ρ_0 the air density, c_0 the speed of sound, and $S = ab$ the cross-sectional area of the chamber.

Defining the volume velocity $v_i = A_i u_i$, and

$$E_{ii'} = \frac{(-1)}{A_i A_{i'}} \sum_{mpn} \frac{e_m e_p e_n}{l} \left(\frac{k}{k_{mpn}^2 - k^2}\right) \times \cos\left(\frac{p\pi y_{i'o}}{l}\right) \cos\left(\frac{p\pi y_{io}}{l}\right) C_{mi'} C_{ni'} C_{mi} C_{ni} \tag{3-29}$$

the averaged acoustic pressures on the surfaces of the two ‘‘pistons’’ may be written as

$$\bar{p}_{ii'} = (-1)^{i'} jZ_0 v_{i'} E_{ii'} \tag{3-30}$$

For the condition $i = i'$ Eq. (3-29) reduces to

$$E_{ii} = \frac{(-1)}{A_i^2} \sum_{mpn} \frac{e_m e_p e_n}{l} \left(\frac{k}{k_{mpn}^2 - k^2}\right) \cos^2\left(\frac{p\pi y_{io}}{l}\right) C_{mi}^2 C_{ni}^2 \quad i = 1 \text{ or } 2 \tag{3-31}$$

From Eq. (3-29) it may be noted that $E_{ii'} = E_{i'i}$, which shows that these values are independent of the inlet and outlet port (or piston) positions. In other words, E-functions satisfy the reciprocity principle.

The total sound pressure acting on the inlet and outlet ports or pistons can be expressed as

$$\bar{p}_1 = \bar{p}_{11} + \bar{p}_{12} = -jv_1 Z_0 E_{11} + jv_2 Z_0 E_{12} \tag{3-32}$$

and

$$\bar{p}_2 = \bar{p}_{22} + \bar{p}_{21} = jv_2 Z_0 E_{22} - jv_1 Z_0 E_{21} \tag{3-33}$$

The transfer matrix of the rectangular expansion chamber of Figure 1, relating the acoustic state variables at the inlet and outlet may now be written as

$$\begin{bmatrix} \bar{p}_1 \\ v_1 \end{bmatrix} = \begin{bmatrix} T_{11} & T_{12} \\ T_{21} & T_{22} \end{bmatrix} \begin{bmatrix} \bar{p}_2 \\ v_2 \end{bmatrix} \tag{3-34}$$

Making use of Eqs. (3-32) and (3-33), the four-pole parameters $T_{ii'}$ can be written in terms of the E-functions as follows [13]:

$$\begin{aligned} T_{11} &= \left(\frac{\bar{p}_1}{\bar{p}_2} \right)_{v_2=0} = \frac{E_{11}}{E_{12}} \\ T_{12} &= \left(\frac{\bar{p}_1}{v_2} \right)_{\bar{p}_2=0} = jZ_0 \left(E_{12} - \frac{E_{11}E_{22}}{E_{12}} \right) \\ T_{21} &= \left(\frac{v_1}{\bar{p}_2} \right)_{v_2=0} = j\left(E_{12}Z_0\right)^{-1} \\ T_{22} &= \left(\frac{v_1}{v_2} \right)_{\bar{p}_2=0} = \frac{E_{22}}{E_{12}} \end{aligned} \tag{3-35}$$

Once four-pole parameters are found, TL can be calculated by the use of Eq. (3-2).

3.1.4 Reverse-flow configuration

Generally in this configuration the inlet and outlet ports are on the same face and the flow direction is reversed as shown in Figure 1. The quantities required to calculate the four-pole parameters in the reverse flow are E_{11}, E_{12} and E_{22} which can be calculated from Eqs. (3-29) and (3-31).

$$E_{11} = \frac{(-1)}{(a_1 b_1)^2} \sum_{mpn} \frac{e_m e_p e_n}{l} \left(\frac{k}{k_{mpn}^2 - k^2} \right) C_{m1}^2 C_{n1}^2 \tag{3-36}$$

$$E_{12} = \frac{(-1)}{(a_1 b_1)(a_2 b_2)} \sum_{mpn} \frac{e_m e_p e_n}{l} \left(\frac{k}{k_{mpn}^2 - k^2} \right) C_{m1} C_{n1} C_{m2} C_{n2} \tag{3-37}$$

$$E_{22} = \frac{(-1)}{(a_2 b_2)^2} \sum_{mpn} \frac{e_m e_p e_n}{l} \left(\frac{k}{k_{mpn}^2 - k^2} \right) C_{m2}^2 C_{n2}^2 \tag{3-38}$$

3.2 Eigen expansion method

In this theory, suggested by Ih [13], the chamber is modeled as a piston-driven tube where the pistons are fluctuating in a predetermined manner. The four-pole parameters are explicitly given in a very simple form. The basic idea for this model stems from the fact that plenum chambers are in general regular in shape, which permits the use of series of orthogonal eigenfunctions. It is idealized insofar as it is assumed that the chamber has no acoustic sources inside it, the walls are not yielding and the effect of mean flow is excluded. By using the transfer matrix implemented by appropriate truncation of the acoustic modal terms, the transmission loss or insertion loss for any rectangular plenum chamber of flow-reversal types can be accurately predicted.

It is assumed that the chamber has no sources inside it and that all the boundaries except the piston are acoustically hard walls. Initially, the fluid medium contained is assumed to be stationary, homogeneous, inviscid and non-heat-conducting. With these assumptions, the linearized three-dimensional wave equation is

$$\nabla^2\phi = \left(1/c^2\right)\partial^2\phi/\partial t^2 \tag{3-39}$$

and its solution, $\phi(x,y,z,t)$, is the velocity potential of the acoustically perturbed fluid; c is the speed of sound in the medium at rest and ∇^2 is the three-dimensional Laplacian operator in a Cartesian co-ordinate system.

3.2.1 A rectangular tube driven by a rectangular piston

The piston in Figure 2 is assumed to be fluctuating back and forth in a steady state

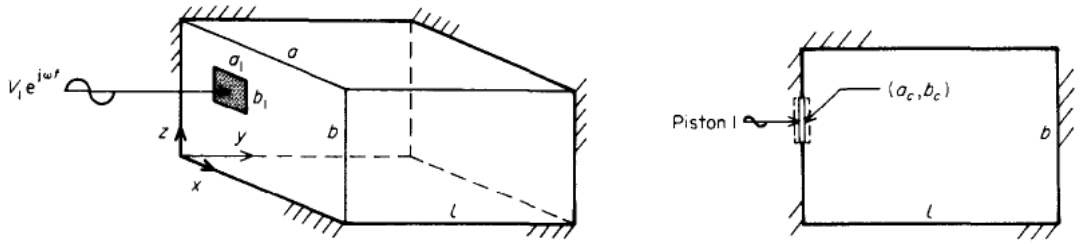

Figure 2: A rectangular plenum chamber harmonically excited by a rectangular piston uniformly moving back and forth

simple harmonic motion. A general solution to Eq (3-39) can be written as

$$\phi(x,y,z,t) = \phi(x,y,z)\exp(j\omega t) \tag{3-40}$$

Where

$$\phi(x,y,z) = \sum_{m=0}^{\infty}\sum_{n=0}^{\infty}\cos(m\pi x/a)\cos(n\pi z/b)\left\{A_{mn}\exp\left(jk_y^+ y\right) + B_{mn}\exp\left(jk_y^- y\right)\right\} \tag{3-41}$$

Here, rigid boundary conditions in the x- and z-directions have been assumed, a is the width of the chamber in the x-direction, b is the height of the chamber in the z-

direction, *m* and n are acoustic mode numbers in the x- and z-directions, respectively, and *A* and *B* are as yet undetermined coefficients to be determined by the boundary conditions in the y-direction. The *k*'s are the y-direction, or axial, wavenumbers with the component waves propagating (or evanescing) in the direction corresponding to the superscript.
From the relation

$$k_x^2 + k_y^2 + k_z^2 = k^2 \tag{3-42}$$

the wave number k_y or equivalently k_{mn} is given by

$$k_y^{\pm} = \mp\sqrt{k^2 - (m\pi/a)^2 - (n\pi/b)^2} \equiv \mp k_y \tag{3-43}$$

Using this, and from the boundary condition

$$-\partial\phi/\partial y\,|_{y=l} = 0 \tag{3-44}$$

One obtains

$$B_{mn} = A_{mn}\exp(-2jk_y l) \tag{3-45}$$

where *l* is the axial length of the chamber. Substituting Eq (3-45) into Eq (3-41), one obtains a new expression for $\phi(x,y,z)$:

$$\phi(x,y,z) = \sum_{m=0}^{\infty}\sum_{n=0}^{\infty} 2A_{mn}\cos(m\pi x/a)\cos(n\pi z/b)\cos\{k_y(l-y)\}\exp(-jk_y l) \tag{3-46}$$

Another boundary condition at the inlet side can be stated as

$$-\partial\phi/\partial y\,|_{y=0} = V_1 f(x,z) \tag{3-47}$$

where V_i is the root-mean-square, or average, particle velocity at the input piston and $f(x,z)$ is the Heaviside unit step function, which is 1 on the input piston and 0 at other positions on the end plate at the driving side. This means that the system is equivalent to an open circuit as an electrical analogy. Substituting Eq (3-46) into Eq (3-47) and operating on both sides by $\int_0^a\int_0^b \cos(m'\pi x/a)\cos(n'\pi z/b)\,dxdz$ to utilize the orthogonality property of eigenfunctions, one obtains

$$\iint_{piston} V_1 \cos(m'\pi x/a)\cos(n'\pi z/b)\,dxdz$$
$$= \sum_{m,m'=0}^{\infty}\sum_{n,n'=0}^{\infty} 2A_{mn}\int_0^a\int_0^b \cos(m\pi x/a)\cos(n\pi z/b)\cos(m'\pi x/a)\cos(n'\pi z/b)\,dxdz \quad (3\text{-}48)$$
$$\times \sin(k_y l)\exp(-jk_y l)$$

The coefficient A_{mn} can be easily derived by integrating the rearranging Eq (3-48). Consequently, the velocity potential due to the motion of piston 1 can be constructed as follows :

$$\begin{aligned}\phi_1(x,y,z) = -V_1\Bigg[&\frac{a_1 b_1}{ab}\frac{\cos k(l-y)}{k\sin kl}\\ &+\Bigg\{\sum_m{}'\frac{2}{\nu_{m0}}\frac{b_1}{b}\frac{1}{m\pi}\sin\frac{m\pi a_1}{2a}\cos\frac{m\pi a_c}{a}\cos\frac{m\pi x}{a}\\ &+\sum_n{}'\frac{2}{\nu_{0n}}\frac{a_1}{a}\frac{1}{n\pi}\sin\frac{n\pi b_1}{2b}\cos\frac{n\pi b_c}{b}\cos\frac{n\pi z}{b}\\ &+\sum_m{}'\sum_n{}'\frac{2}{\nu_{mn}}\frac{1}{mn\pi^2}\sin\frac{m\pi a_1}{2a}\cos\frac{m\pi a_c}{a}\sin\frac{n\pi b_1}{2b}\\ &\times\cos\frac{n\pi b_c}{b}\cos\frac{m\pi x}{a}\cos\frac{n\pi z}{b}\Bigg\}\frac{\cos k_y(l-y)}{k_y\sin k_y l}\Bigg]\end{aligned} \quad (3\text{-}49)$$

Here, the primes on the summation sign mean that the m =0 and/or n= 0 modes are excluded, (a_c, b_c) are the co-ordinates of the centre of the input piston, and a_1 and b_1, denote the piston size, as shown in Figure 2. The ν's come from evaluating Eq (3-48), where the integration on the right side is a suitable form for the application of the orthogonality of the eigenfunctions. If one denotes the double integration term of the right side of Eq (3-48) as *I*, then $I = \nu_{mn} ab$, resulting in:

$$\nu_{00} = 1, \qquad \nu_{m0} = \nu_{0n} = 1/2 \qquad \nu_{mn} = 1/4 \quad (3\text{-}50)$$

The first term in Eq (3-49) denotes the plane wave mode contribution, and the rest on the right side are higher order mode contributions.

From the linearized momentum equation, the sound pressure at a point inside the chamber due to the steady harmonic excitation of the input piston is given by

$$p_1(x,y,z) = j\omega\rho_0\phi_1(x,y,z) \quad (3\text{-}51)$$

where ρ_0 is the density of the unperturbed medium.

3.2.2 Transfer matrix derivation

On a rectangular area *i'* with area $S_{i'}$ in the *x*-*z* plane at an axial distance *y* from the input piston *i*, the average pressure is

$$\bar{p}_{i'i} = \frac{1}{S_{i'}} \iint_{S_t} p_i dx dz \tag{3-52}$$

where $\bar{p}$ denotes the averaged acoustic pressure and the subscript *i'i* signifies the value at the area *i'* caused by the action of the piston *i*.

If another piston *i'* is located on the same plane as piston 1, as depicted in Figure 2, the averaged acoustic pressure on the piston i due to its own motion is[1]

$$\begin{aligned} \bar{p}_{ii} &= (-1)^i jU_i Z_0 \left[\frac{1}{\tan kl} + \left(\frac{ab}{a_i b_i} \right)^2 \left\{ \sum_m{}' \frac{1}{\nu_{m0}} \left(\frac{2}{m\pi} \right)^2 \left(\frac{b_i}{b} \right)^2 \psi_1^2 \right. \right. \\ &\left. \left. + \sum_n{}' \frac{1}{\nu_{0n}} \left(\frac{2}{n\pi} \right)^2 \left(\frac{a_i}{a} \right)^2 \psi_2^2 + \sum_m{}' \sum_n{}' \frac{1}{\nu_{mn}} \left(\frac{4}{mn\pi^2} \right)^2 \psi_2^2 \psi_1^2 \right\} \frac{k}{k_y \tan k_y l} \right] \\ &\equiv (-1)^i jU_i Z_0 E_{ii}, \qquad i = 1 \ or \ 2 \end{aligned} \tag{3-53}$$

where U_i is the volume velocity of the piston *i* (that is, $U_i = a_i b_i V_i$), Z_0 is the acoustic impedance of the chamber in the y-direction (i.e., $Z_0 = \rho_0 c / ab$), E_{ii} denotes the terms in the square brackets, and, for notational simplicity,

$$\psi_1 = \sin(m\pi a_i / 2a)\cos(m\pi a_{ci} / a), \quad \psi_2 = \sin(n\pi b_i / 2b)\cos(n\pi b_{ci} / b) \tag{3-54}$$

If another piston or port is located on the same plane as piston 1, as shown in Figure 3, then the system is a flow-reversal type and the interacting average sound

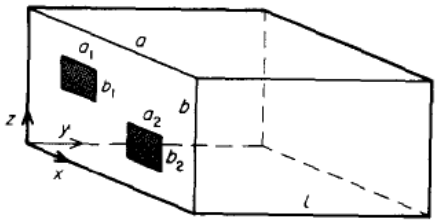

Figure 3: End-in/end-out configurations with rectangular inlet and outlet: a flow-reversal

pressure is given by

$$\bar{p}_{i'i} = (-1)^i jU_i Z_0 \left[\frac{1}{\tan kl} + \left(\frac{ab}{a_i b_i} \right) \left(\frac{ab}{a_{i'} b_{i'}} \right) \left\{ \sum_m{}' \frac{1}{\nu_{m0}} \left(\frac{2}{m\pi} \right)^2 \left(\frac{b_i}{b} \right) \left(\frac{b_{i'}}{b} \right) \psi_1 \psi'_1 \right. \right. \tag{3-55}$$

[1] The first plus sign in Eq. (3-53) is missing in the original paper [13].

$$+\sum_{n}^{'}\frac{1}{\nu_{0n}}\left(\frac{2}{n\pi}\right)^2\left(\frac{a_i}{a}\right)\left(\frac{a_{i'}}{a}\right)\psi_2\psi'_2$$
$$+\sum_{m}^{'}\sum_{n}^{'}\frac{1}{\nu_{mn}}\left(\frac{4}{mn\pi^2}\right)^2\psi_2\psi'_2\psi_1\psi'_1\left\{\frac{k}{k_y\tan k_y l}\right]$$
$$\equiv(-1)^i\, jU_i Z_0 E_{i'i}, \qquad i=1 \text{ and } i'=2 \quad \text{or} \quad i=2 \text{ and } i'=1$$

Where

$$\psi'_1=\sin(m\pi a'_i/2a)\cos(m\pi a_{ci'}/a), \qquad \psi'_2=\sin(n\pi b'_i/2b)\cos(n\pi b_{ci'}/b) \tag{3-56}$$

In Eq (3-55) one can easily find that the terms in the square brackets do not depend on the relative positions of the inlet and outlet ports, so that $E_{i'i}=E_{ii'}$.

The total acoustic potential field can be obtained by superposing the two velocity potentials in accordance with the motion of the two pistons: i.e., $\phi=\phi_1+\phi_2$. Therefore, the total sound pressure acting on the piston can be written as

$$\begin{aligned}\bar{P}_1&=\bar{p}_{11}+\bar{p}_{12}=-jZ_0(U_1E_{11}-U_2E_{12}),\\ \bar{P}_2&=\bar{p}_{21}+\bar{p}_{22}=-jZ_0(U_1E_{21}-U_2E_{22})\end{aligned} \tag{3-57}$$

The transfer matrix can be written as

$$\begin{bmatrix}\bar{p}_1\\ U_1\end{bmatrix}=\begin{bmatrix}T_{11} & T_{12}\\ T_{21} & T_{22}\end{bmatrix}\begin{bmatrix}\bar{p}_2\\ U_2\end{bmatrix} \tag{3-58}$$

where the T_{ii}'s are the four-pole parameters, and can be found from Eq. (3-57) and the result would be the same as Eq. (3-35).

Once four-pole parameters are found, TL can be calculated by the use of Eq. (3-2).

3.3 Eigen expansion method for cylindrical chambers [1]

3.3.1 Piston-driven tube model

In this part in addition to the assumptions of part 3.2, it's assumed that axial cross-section of the chamber is uniform. The locations of the inlet and outlet are offset from the center of the chamber, in general. With these assumptions, the three-dimensional linear wave equation is given by

$$\nabla^2\phi=(1/c^2)\partial^2\phi/\partial t^2 \tag{3-59}$$

where the solution $\phi(r,\theta,z,t)$, is the velocity potential of the acoustically perturbed fluid, *c* is the speed of sound in the medium at rest and ∇^2 is the three-dimensional Laplacian operator in cylindrical co-ordinates defined as:

$$\nabla^2 = \partial^2/\partial r^2 + (1/r)\partial/\partial r + (1/r^2)\partial^2/\partial\theta^2 + \partial^2/\partial z^2 \tag{3-60}$$

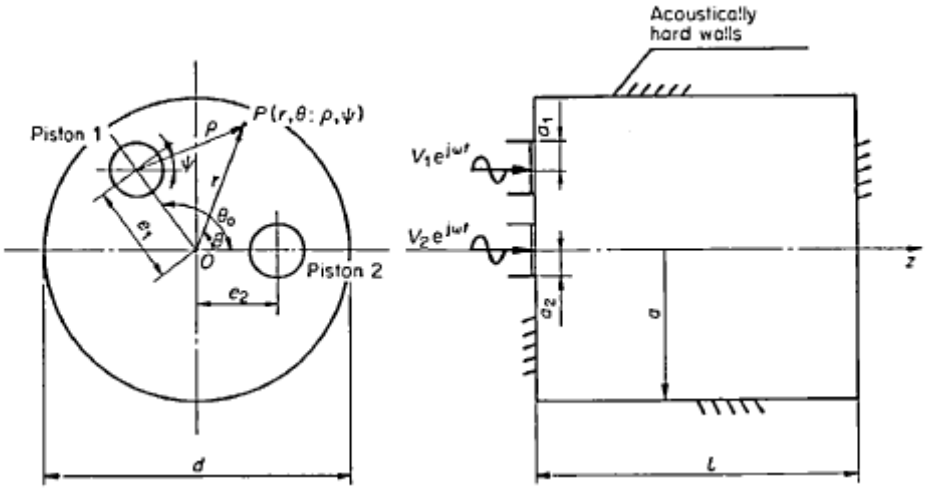

Figure4: Geometric description of a model of a reversing chamber mufflers illustrating the relationship between circular coordinates for an aperture (inlet or outlet) and the chamber.

The given geometry is analogous to a circular tube excited by a hypothetical plane circular piston which may be eccentrically located inlet or outlet, as shown in Figure4, fluctuating back and forth in a steady state simple harmonic motion.

Separating the variables leads to four second order ordinary differential equations, and the general eigenfunction solution to equation Eq. (3-59) can then be written as

$$\phi(r,\theta,z,t) = 2^{1/2}\Phi(r,\theta,z)\exp(jwt) \tag{3-61}$$

or

$$\Phi(r,\theta,z) = \sum_{n=0}^{\infty}\sum_{m=0}^{\infty} J_n\left(k_{r_{mn}} r\right)\cos n\theta\left\{A_{nm}\exp\left(jk_{z_{nm}}^{-} z\right) + B_{nm}\exp\left(jk_{z_{nm}}^{+} z\right)\right\} \tag{3-62}$$

where the coefficient $2^{1/2}$ is factored out to make a root-mean-squared value, *w* is the radian frequency, J_n is the Bessel function of the first kind of order n, n is the circumferential mode number, m is the radial mode number, the *k's* are the wave numbers in the indicated directions, *A* and *B* are undetermined constants, and the superscripts indicate the directions of propagation $(\pm z)$.

The values of the *k's*, *A* and *B* are determined by the following boundary conditions:

$$\begin{aligned} -\partial\Phi/\partial r\big|_{r=a} &= 0 \\ -\partial\Phi/\partial z\big|_{z=l} &= 0 \\ -\partial\Phi/\partial z\big|_{z=0} &= (-1)^{i-1} V_i f(r,\theta) \equiv F(r,\theta) \end{aligned} \tag{3-63}$$

Here V_i is the amplitude of the uniform particle velocity at an input piston, and $f(r,\theta)$ is the Heaviside unit step function which is 1 on the input piston and 0 at the other position on the end plate. The last boundary condition implies that only one input piston is considered at a time, with the other piston(s) assumed rigid. This allows the piston velocities to be determined independently in what follows.

From the radial boundary condition prescribed in Eq. (3-63a), one obtains

$$dJ_n\left(k_{r_{nm}} r\right)/\, dr\big|_{r=a} = 0 \tag{3-64}$$

For conciseness, the roots, $k_{r_{nm}} a$, satisfying Eq. (3-64), are denoted henceforth by λ_{nm} some values of which are listed in reference [22].

Combination of Eqs. (3-62) and (3-63b) yields

$$B_{nm} = -A_{nm}\left(k^-_{z_{nm}} / k^+_{z_{nm}}\right)\exp\left\{jl\left(k^-_{z_{nm}} - k^+_{z_{nm}}\right)\right\} \tag{3-65}$$

From the relationship

$$k_z^2 + k_r^2 = k^2 \tag{3-66}$$

where $k = w/c$, the wave number k.. is given by

$$k^{\mp}_{z_{nm}} = \pm k\left\{1 - \left(\lambda_{nm}/ka\right)^2\right\}^{1/2} \tag{3-67}$$

Thus, the substitution of Eqs. (3-65) and (3-67) into Eq. (3-62) leads to a new expression for Φ

$$\Phi(r,\theta,z) = \sum_{n=0}^{\infty}\sum_{m=0}^{\infty} J_n\left(\lambda_{nm} r/a\right)\cos n\theta\, A_{nm}\left\{\exp\left(jk^-_{z_{nm}} z\right) + \exp\left(jk^-_{z_{nm}}\left(2l - z\right)\right)\right\} \tag{3-68}$$

From now on, the minus sign superscript of k_z^- is omitted for notational simplicity, the parameter k_z appearing in the following being equal to k_z^- defined in Eq. (3-67).

To fit the third boundary condition, a partial differentiation of Eq. (3-68) with respect to z and insertion into Eq. (3-63c) yields

$$\begin{aligned} &-\partial\Phi/\partial z\big|_{z=0} = \\ &-\sum_{n=0}^{\infty}\sum_{m=0}^{\infty} 2A_{nm}k_{z_{nm}} J_n\left(\lambda_{nm} r/a\right)\cos n\theta \times \exp\left(jk_{z_{nm}} l\right)\sin\left(k_{z_{nm}} l\right) = F(r,\theta) \end{aligned} \tag{3-69}$$

Eq. (3-69) can be seen to be composed of a first order combination of the Bessel and the cosine function; hence the method of Fourier-Bessel expansion [23] of $F(r,\theta)$ can be applied. Comparing the expanded result with Eq. (3-69) gives the coefficients A_{nm}.Consequently, the velocity potential is given by collecting these results:

$$\Phi_i(r,\theta,z) = (-1)^i \frac{V_i}{\pi a^2}\left[\frac{\cos k(l-z)}{k\sin kl}\right.$$
$$\times \iint_{pistoni} rf(r,\theta)drd\theta + \sum_n{}' \sum_m{}' \frac{\cos k_{z_{nm}}(l-z)}{k_{z_{nm}}\sin k_{z_{nm}} l} \frac{J_n(\lambda_{nm} r/a)\cos n\theta}{(1-n^2/\lambda_{nm}^2)J_n^2(\lambda_{nm})} \quad (3\text{-}70)$$
$$\left.\times \iint_{pistoni} rf(r,\theta)J_n(\lambda_{nm} r/a)\cos n\theta drd\theta\right], \qquad i = 1 \text{ or } 2$$

The primes on the summation sign mean that the plane wave contribution (n =0 and m = 0) is excluded.

The double integration in Eq. (3-70) subject to the boundary condition prescribed in Eq. (3-63c) can be accomplished by using Graf's addition formula for the Bessel functions [23]. After transforming the cylindrical wave functions associated with the co-ordinates of the chamber to those of the piston, the integrations in Eq. (3-70) can be performed readily. The addition formula is

$$J_n(\lambda_{nm} r/a)\cos n\theta = \sum_{p=-\infty}^{\infty} J_{n+p}(\lambda_{nm}\rho/a)J_p(\lambda_{nm} e_i/a)\cos\{(n+p)\psi - p\theta_0\} \quad (3\text{-}71)$$

where (ρ,ψ) is a local co-ordinate system associated with the piston, e_i is the-distance between the centers of the piston and chamber, and θ_0 is the angular distance of the piston from the datum line.

After using the Eq. (3-71), the velocity potential in Eq. (3-70) becomes

$$\Phi_i(r,\theta,z) = (-1)^i \frac{V_i \pi a_i^2}{\pi a^2}\left[\frac{\cos k(l-z)}{k\sin kl}\right.$$
$$\left. + 2\left(\frac{a}{a_i}\right)\sum_n{}' \sum_m{}' \frac{\cos k_{z_{nm}}(l-z)}{k_{z_{nm}}\sin k_{z_{nm}} l} \frac{J_{-n}(\lambda_{nm} e_i/a)J_1(\lambda_{nm} a_i/a)}{(1-n^2/\lambda_{nm}^2)J_n^2(\lambda_{nm})\lambda_{nm}}\right] \qquad i = 1 \text{ or } 2 \quad (3\text{-}72)$$

In this expression it can be seen that the first term on the right-hand side of Eq. (3-72) denotes the plane wave or fundamental mode contribution, and the terms in the summations are the higher order mode contributions.

From the linearized momentum equation, the sound pressure field due to the steady harmonic excitation of the input piston is given by

$$p_i(r,\theta,z) = jw\rho_0\Phi_i(r,\theta,z) \tag{3-73}$$

where ρ_0 is the density of the unperturbed fluid medium.

3.3.2 Transmission or transfer matrix

On a circular area *i'* with radius $a_{i'}$ in the (r,θ)-plane at an axial distance *z* from the input piston *i*, the centre of which is a distance $e_{i'}$ from the centre of the chamber cross-section the average pressure is

$$\bar{p}_{i'i}\frac{1}{\pi a_{i'}^2}\iint_{area\,i'} p_i r dr d\theta \tag{3-74}$$

where the bar above *p* means the averaged quantity and the subscripts *i'i,* in proper sequence, signify the quantity at the area *i'* caused by the action of the piston *i*.

Eq. (3-74) includes the double integration procedure of the cylindrical wave functions, as encountered in Eq. (3-70). By proceeding as before, the addition formula as in Eq. (3-71) can be applied to the combination of Eqs. (3-72) to (3-74): thus,

$$\begin{aligned}\bar{p}_{i'i}(e_{i'},\theta_0,z) &= (-1)^{i'}\, jU_i Z\left[\frac{\cos k(l-z)}{\sin kl}\right.\\ &+ 4\left(\frac{a}{a_i}\right)\left(\frac{a}{a_{i'}}\right)\sum_n{}'\sum_m{}' \frac{k\cos k_{z_{nm}}(l-z)}{k_{z_{nm}}\sin k_{z_{nm}} l}\\ &\left.\times \frac{J_{-n}(\lambda_{nm}e_i/a)J_1(\lambda_{nm}a_i/a)}{(1-n^2/\lambda_{nm}^2)J_n^2(\lambda_{nm})\lambda_{nm}^2} J_{-n}(\lambda_{nm}e_{i'}/a)J_1(\lambda_{nm}a_{i'}/a)\cos n\theta_0\right]\end{aligned} \tag{3-75}$$

Here *Ui* is the volume velocity of the piston *i* $(U_i = \pi a_i^2 V_i)$, and Z is the acoustic impedance of the chamber $Z = \rho_0 c/\pi a^2$.

If the area *i'* is taken to be that of the input piston itself, then, from Eq. (3-75), the average sound pressure acting on the input piston due to its own motion is

$$\bar{p}_{ii}\left(e_{i'},0,0\right)=\left(-1\right)^{i}\,jU_{i}Z\Bigg[\cot kl+\left(\frac{2a}{\lambda_{nm}a_{i}}\right)^{2}\sum_{n}{}'\sum_{m}{}'\frac{k\cot k_{z_{nm}}l}{k_{z_{nm}}}\times$$
$$\frac{J_{n}^{2}\left(\lambda_{nm}e_{i}/a\right)J_{1}^{2}\left(\lambda_{nm}a_{i}/a\right)}{\left(1-n^{2}/\lambda_{nm}^{2}\right)J_{n}^{2}\left(\lambda_{nm}\right)\lambda_{nm}^{2}}\Bigg]\equiv\left(-1\right)^{i}\,jU_{i}ZE_{ii},\quad i=1\;or\;2. \tag{3-76}$$

If the area i' in Eq. (3-75) is, in turn, put equal to that of another input piston, assumed motionless, the interacting average sound pressure is given by

$$\bar{p}_{i'i}\left(e_{i'},\theta_{0},0\right)=\left(-1\right)^{i'}\,jU_{i}Z\Bigg[\cot kl+4\left(\frac{a}{a_{i}}\right)\left(\frac{a}{a_{i'}}\right)\sum_{n}{}'\sum_{m}{}'\frac{k\cot k_{z_{nm}}l}{k_{z_{nm}}}$$
$$\times\frac{J_{1}^{2}\left(\lambda_{nm}a_{i}/a\right)J_{1}^{2}\left(\lambda_{nm}a_{i'}/a\right)}{\left(1-n^{2}/\lambda_{nm}^{2}\right)J_{n}^{2}\left(\lambda_{nm}\right)\lambda_{nm}^{2}}J\;\left(\lambda_{nm}e_{i}/a\right)J_{n}\left(\lambda_{nm}e_{i'}/a\right)\cos n\theta_{0}\;\Bigg] \tag{3-77}$$
$$\equiv\left(-1\right)^{i'}\,jU_{i}ZE_{i'i},\qquad i=1\;and\;i'=2,or\;i=2\;and\;i'=1$$

so that $E_{12}=E_{21}$ In Eqs (3-76) and (3-77), E represents the terms in the bracket.

The total acoustic field due to the presence of two input pistons, i.e., inlet and outlet, is a superposed result of the two velocity potentials ascribed to the motion of each of these pistons,

$$\Phi=\Phi_{1}+\Phi_{2} \tag{3-78}$$

where the index 1 denotes that the quantity is related to the inlet and 2 to the outlet. Accordingly, the total sound pressure acting on piston i can be expressed as

$$\bar{P}_{i}=\bar{p}_{ii}\left(e_{i},0,0\right)+\bar{p}_{ii'}\left(e_{i},\theta_{0},0\right)=\left(-1\right)^{i}\,jZ\left(U_{i}E_{ii}+U_{i'}E_{ii'}\right),\qquad i=1\;or\;2, \tag{3-79}$$

where the first term on the right-hand side stands for the pressure caused by the axial vibration of piston i itself and the second the interaction pressure caused by the piston i'.

The transmission or transfer matrix can again be written as Eq. (3.1) where the T_{ii}'s are the four-pole parameters, and can be found from Eq. (3-79) and the result would be the same as Eq. (3-35). Once four-pole parameters are found, TL can be calculated by the use of Eq. (3-2).

4 FE modeling and calculation of TL and TM

FE modeling is done by COMSOL (Pressure Acoustics) to calculate TL and TM of a desired chamber. As the first step chamber's geometry is modeled and 4 "Domain Point Probes" are used in the ducts to pick up acoustic pressure, see Figure 5 and Figure 20. Afterwards 'Air' is selected to fill in the chamber as a linear elastic fluid with following properties:

Temperature	293.15 K
Density	1.21 kg/m^3
Sound velocity	343 m/s
Absolute pressure	1 atm

All the boundaries of the geometry are considered rigid except for inlet and outlet ports. At the inlet port, plane wave excitation with frequency sweep starting at 20 Hz and ending at 1 kHz is applied and its amplitude is selected to be 1 Pa. At the outlet port impedance" $\rho_0 c_0 = 411.6 \quad kg\,m^{-2}\,s^{-1}$ " is applied to simulate the anechoic termination condition [16]. Initial values of pressure and pressure time derivative are set to zero. Volume is meshed automatically by free tetrahedral elements with following element size:

maximum element size	40 mm
minimum element size	5 mm

So this mesh is valid up to a frequency of 1426 Hz, based on the assumption of minimum six elements per wavelength.

Here harmonic time dependence is assumed which means that frequency domain approach is suitable for solving the problem.

Once the model is solved by COMSOL, acoustic pressures at 4 microphone points are available to be used for further calculations. The origins of the coordinate systems are at the two surfaces connecting the pipes to the muffler. Subscript "-" or "+" denotes the direction of the wave propagation relative to the coordinate system.

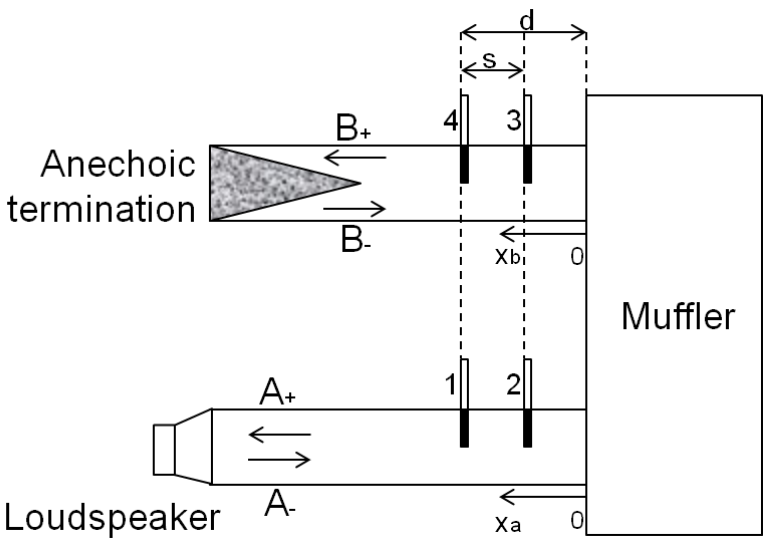

Figure 5: A schematic view of the measurement system and waves

As explained by L. Feng [18], assuming just plane wave propagation in the inlet and outlet ducts, the complex pressure at the measurement positions are

$$\begin{cases} p_1 = A_- \exp(jkx_1) + A_+ \exp(-jkx_1) \\ p_2 = A_- \exp(jkx_2) + A_+ \exp(-jkx_2) \\ p_3 = B_- \exp(jkx_3) + B_+ \exp(-jkx_3) \\ p_4 = B_- \exp(jkx_4) + B_+ \exp(-jkx_4) \end{cases} \tag{4-1}$$

The time factor $\exp(j\omega t)$ is omitted in the expression. The four complex sound pressures can then be obtained as

$$\begin{cases} A_- = \dfrac{p_1 \exp(jks) - p_2}{2j\sin(ks)} \exp(-jkd) \\ A_+ = \dfrac{p_2 - p_1 \exp(-jks)}{2j\sin(ks)} \exp(jkd) \\ B_- = \dfrac{p_4 \exp(jks) - p_3}{2j\sin(ks)} \exp(-jkd) \\ B_+ = \dfrac{p_3 - p_4 \exp(-jks)}{2j\sin(ks)} \exp(jkd) \end{cases} \tag{4-2}$$

In the formula $s = x_1 - x_2 = x_4 - x_3$ and $d = x_1 = x_4$. The formula is valid when $ks \neq n\pi$ where *n* is an integer. The four terms can be related by a scattering matrix as

$$\begin{bmatrix} A_+ \\ B_+ \end{bmatrix} = \begin{bmatrix} r_a & t_{ba} \\ t_{ab} & r_b \end{bmatrix} \begin{bmatrix} A_- \\ B_- \end{bmatrix} \tag{4-3}$$

Where *r* stands for reflection coefficient and *t* represents transmission coefficient. According to the last equation it is clear that the number of unknowns is larger than

the number of equations. However in the cases studied here the silencers are symmetric which means that there is no need for two-load method or two-source method and Eq. (4-3) can be simplified to

$$\begin{bmatrix} A_+ \\ B_+ \end{bmatrix} = \begin{bmatrix} r & t \\ t & r \end{bmatrix} \begin{bmatrix} A_- \\ B_- \end{bmatrix} \tag{4-4}$$

and

$$\begin{bmatrix} r \\ t \end{bmatrix} = \frac{1}{A_-^2 - B_-^2} \begin{bmatrix} A_- A_+ - B_- B_+ \\ A_- B_+ - B_- A_+ \end{bmatrix} \tag{4-5}$$

The formula is based on the assumption $r_a = r_b = r$ and $t_{ab} = t_{ba} = t$ (reciprocity of transmission loss). The sound TL is then obtained as

$$TL = -10 \log\left(|t|^2\right) \tag{4-6}$$

As it will be discussed later Transmission Matrix (TM) is also needed. TM connects the acoustic pressure and volume velocity in the inlet to the same state variables in the outlet and can be defined as:

$$\begin{bmatrix} \hat{p} \\ -\hat{v} \end{bmatrix}_{inlet} = TM \begin{bmatrix} \hat{p} \\ \hat{v} \end{bmatrix}_{outlet} \tag{4-7}$$

Where

$\hat{p}$: Complex pressure at inlet or outlet

$\hat{v}$: Complex volume velocity at inlet or outlet

$TM = \begin{bmatrix} T_{11} & T_{12} \\ T_{21} & T_{22} \end{bmatrix}$: Transmission matrix

TM is very convenient to use when several mufflers are put together and it is calculated as explained by L. Feng [18]

$$\begin{bmatrix} T_{11} & T_{12} \\ T_{21} & T_{22} \end{bmatrix} = \frac{1}{2t} \begin{bmatrix} 1+t^2-r^2 & \rho c\left(1-t^2+r^2+2r\right) \\ \dfrac{\left(1-t^2+r^2-2r\right)}{\rho c} & 1+t^2-r^2 \end{bmatrix} \tag{4-8}$$

In the formula the reciprocity principle for the transmission and reflection coefficient has been used.

5 Results and discussion

5.1 TL and TM elements for rectangular chambers

In this part a rectangular chamber is considered and then it's solved for the calculation of TL and TM by different methods. A sketch of the cross section of the chamber is shown in Figure 6.

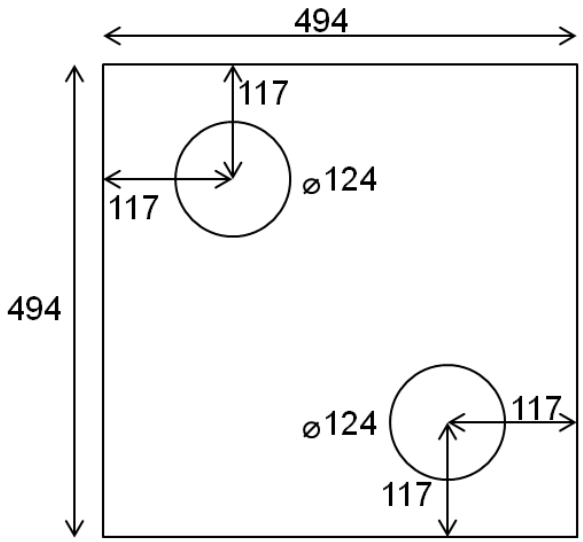

Figure 6: Schematic cross section of the chamber (dimensions in mm).

Figure 7 and Figure 8 compare TL from the two theoretical methods, FEM and measurement for chambers with cross section shown in Figure 6 and 2 different depths of the chamber (100 and 300 mm). Measurement data are provided by Mikael Karlsson. It can be seen that all these results are in a very good agreement. Besides, Lindborg et al. [11] tried to approximate the acoustic characteristic of a shallow flow reversal chamber with simple two port elements like a *large quarter wave resonator* or a *simple pipe* and these results are also included in Figure 7 and Figure 8. The validity range of quarter wave resonator model is well below 100 Hz while a simple pipe model is a good approximation under cut on frequency of the first higher order mode.

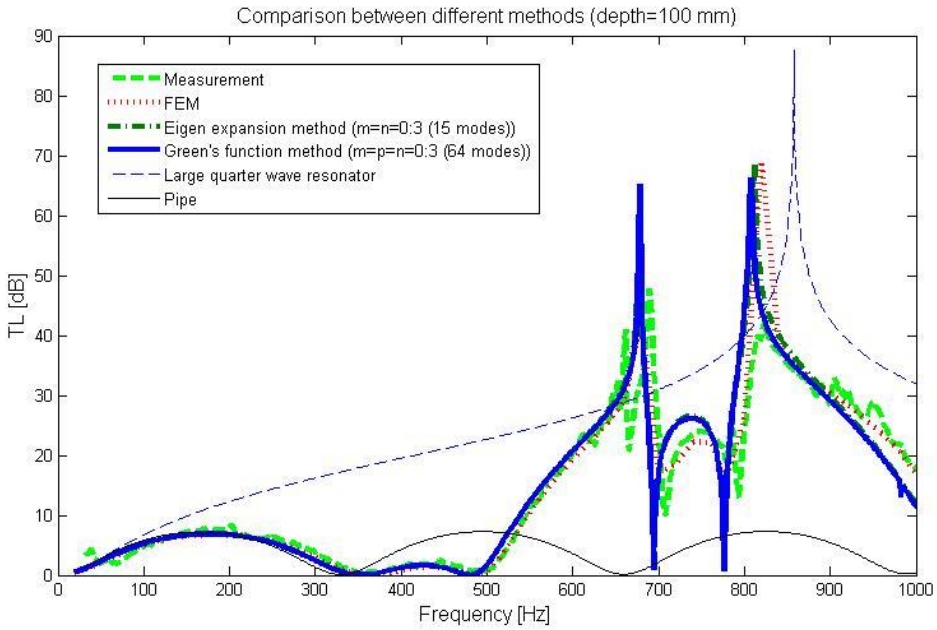

Figure 7

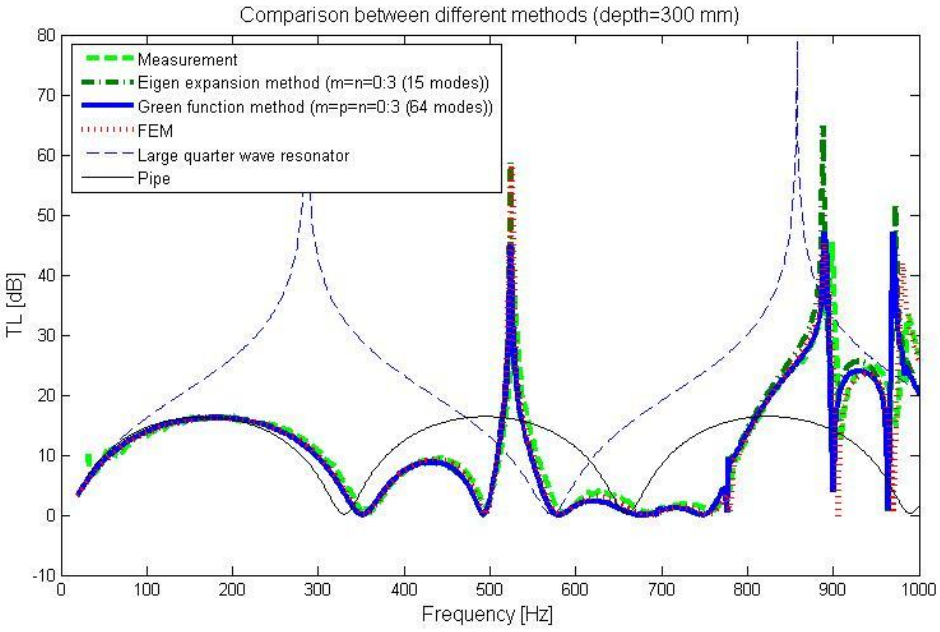

Figure 8

One way to calculate TL of a total exhaust system is to find the TM of each element of the system and then multiply all the TMs to find the total TM. Having the total TM, it would be possible to calculate the total TL by the use of Eq. (3-2). This means that one should not validate the results of TL but also elements of TM should be compared. Figure 9 to Figure 12 show the comparison of TM elements where 15 and 64 modes are considered for Eigen expansion and Green's function methods respectively. It should be mentioned that elements T_{12} and T_{21} are normalized by dividing by Z_2 and multiplying by Z_1 respectively. ($Z_1 = \rho_0 c_0 / S_1$ and $Z_2 = \rho_0 c_0 / S_2$, where $S_1 = a_1 b_1$ and $S_2 = a_2 b_2$)

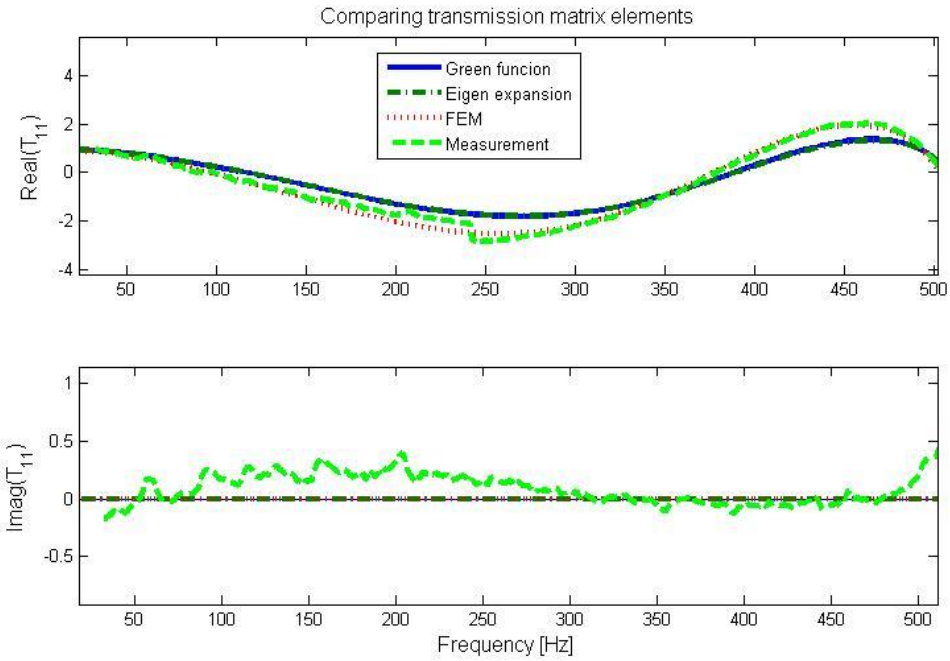

Figure 9

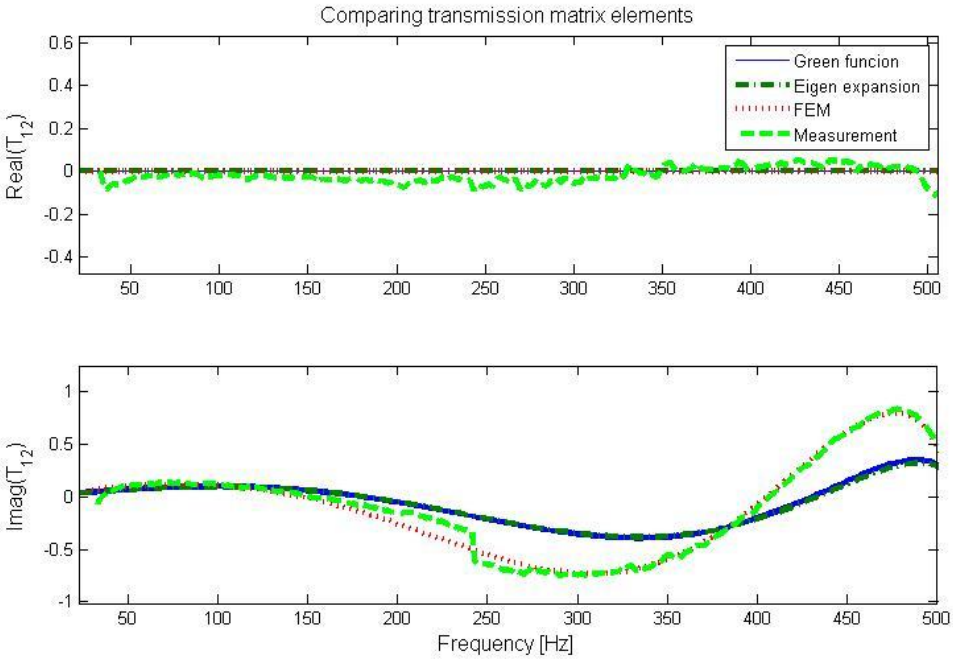

Figure 10

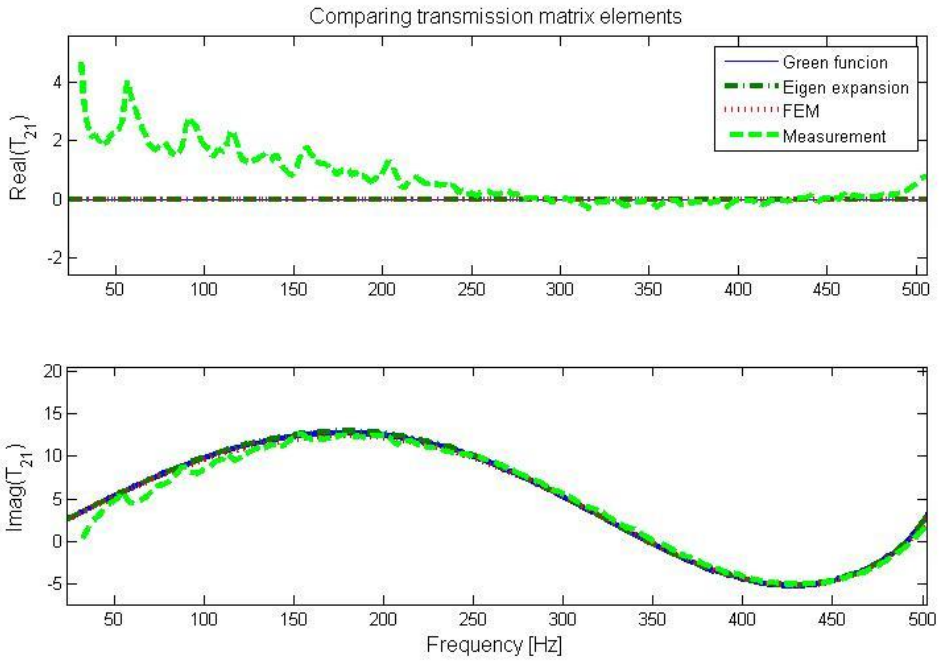

Figure 11

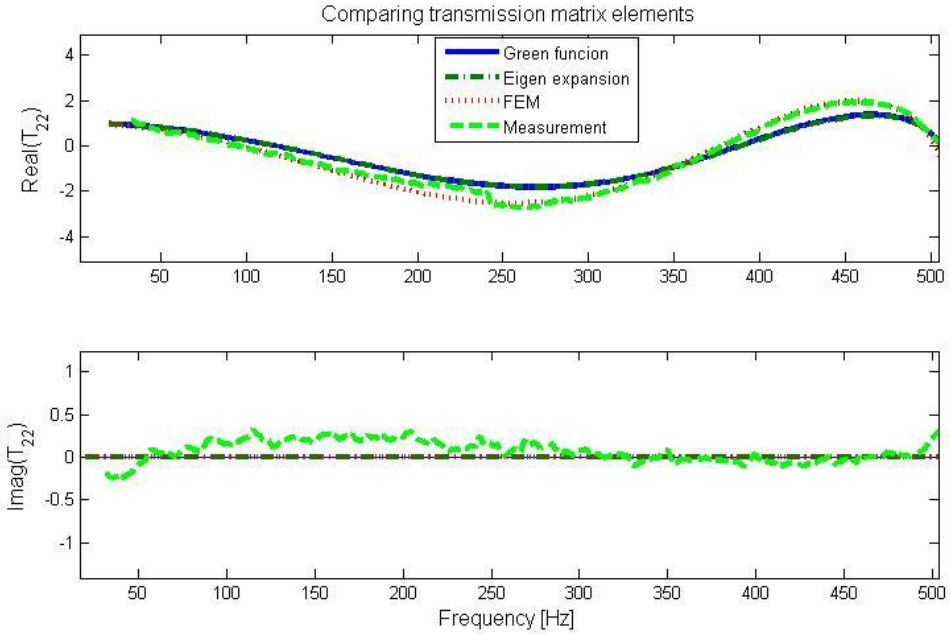

Figure 12

Based on Figure 9 to Figure 12 it can be said that results are generally compatible; however, closer look reveals that results can be divided into 2 groups based on how close they are. FE and measurement results make the first group and the second group is consisted of the two theories. The first group shows the correct solution. The discrepancy between the results may be solved by introducing acoustic length correction of duct extension into the chamber. As far as these theories are used for predicting the TL of a chamber alone, good results can be expected, see Figure 7 and Figure 8. However this discrepancy can result in large error in calculation of total TL for an exhaust system. As an example this error is investigated for a case of an idealized truck silencer in the following section.

It can be noticed that sometimes there is a jump around 240 Hz in the measurement results like first plot of Figure 9. This jump is due to the use of two microphone configurations to cover all the frequency range.

5.2 Idealized truck silencer

To illustrate the effect of errors in the modelling approaches on a practical problem a simple truck silencer configuration is tested. The rectangular chamber with cross section shown in Figure 6 is used as a reactive silencer to which typical length ducts are attached, see Figure 13. In a typical truck installation a one meter pipe routes the exhaust from the turbine to the silencer. After the silencer an endpipe of about 0.4 m is usually a good choice. A real silencer is of course more complicated but this idealised configuration allows us to isolate the effect of the reversal chamber.

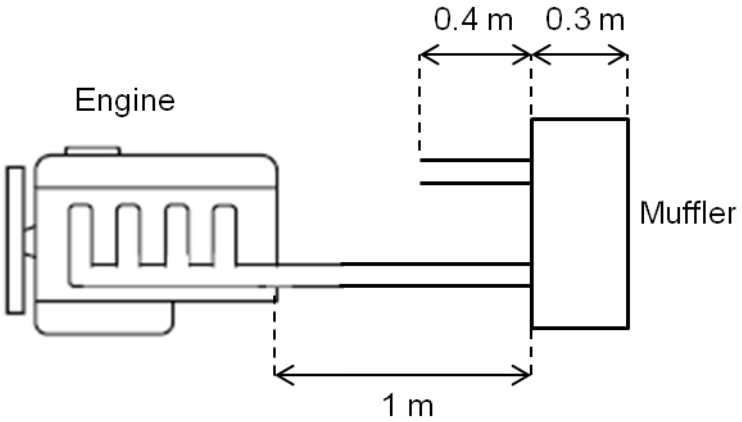

Figure 13: Idealised silencer configuration

The simulations are performed in the linear acoustic multiport code SIDLAB [24]. The transfer matrices obtained from the FEM simulation and Green's function method [16] are imported into the program. The ducts are modelled using simple straight duct elements [19]. The system is terminated by an open end, with an impedance according to the model of Levine & Schwinger [21] The upstream impedance is defined using the impedance model of Peat [25].

Comparing the transmission loss for the reversal chamber alone, Figure 8, FEM and green function method yield similar results. This was expected from the result presented in the derivation of the model. However, when the reversal chamber interacts with the pipes, that is studying insertion loss where the phase becomes important, it is more cumbersome, see Figure 14. Some troughs are shifted considerably in frequency. Perhaps most important is that the low frequency performance is overestimated by green function method, see Figure 15. This frequency range is very critical as for a typical six cylinder heavy duty vehicle the engine firing orders, where most of the acoustic energy is, range from 50-100 Hz. This is usually the most challenging part in the development of a silencer, to provide sufficient damping at these really low frequencies. With this simple demonstration example there is an overestimation of ~5 dB at 70 Hz by the Green's function method. This could be critical in the design stage when different designs are being considered.

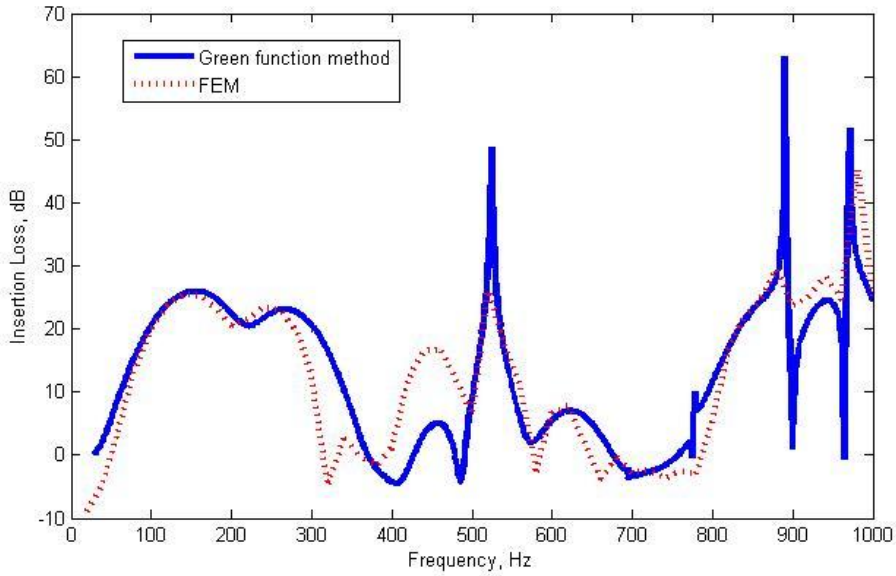

Figure 14: Idealized truck silencer insertion loss calculated for different chamber models

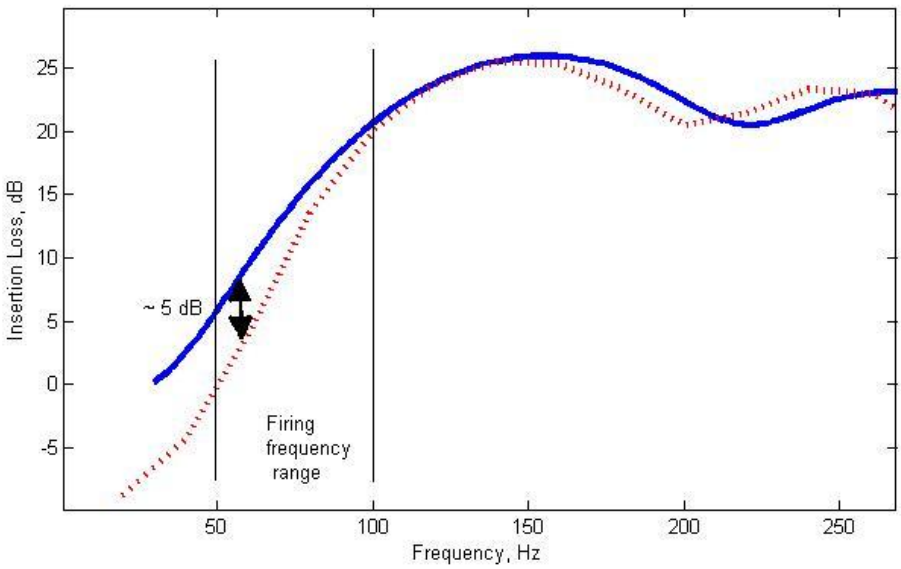

Figure 15: Insertion loss in the critical firing frequency range

5.3 Effect of number of modes in theoretical solutions

Figure 16 and Figure 17 show how by increasing number of modes in the Green's function and Eigen expansion methods respectively, solutions approach to the correct solution from FEM. These plots are for a case of a chamber with cross section according to Figure 6 and depth of the chamber is 300 mm.

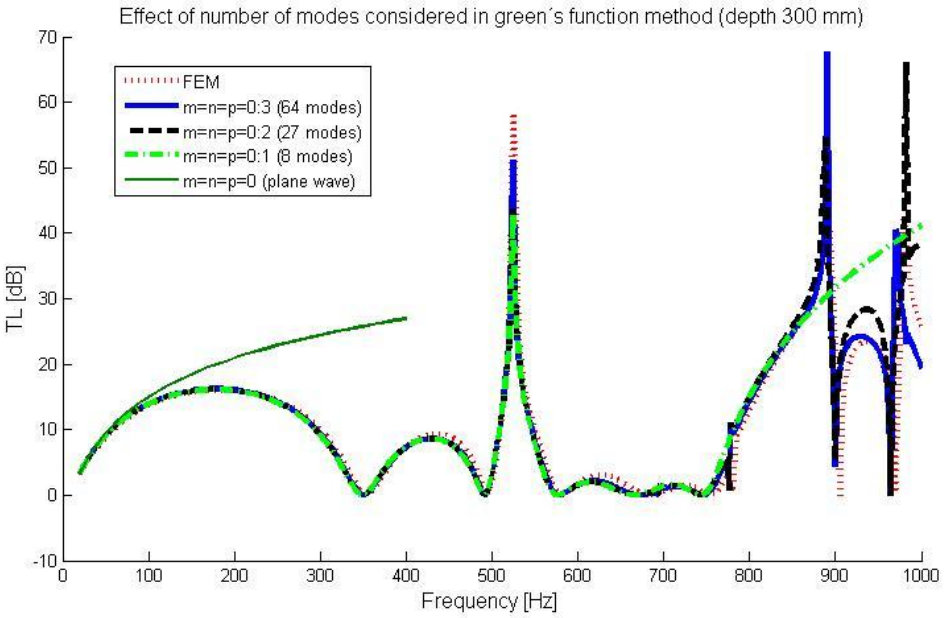

Figure 16

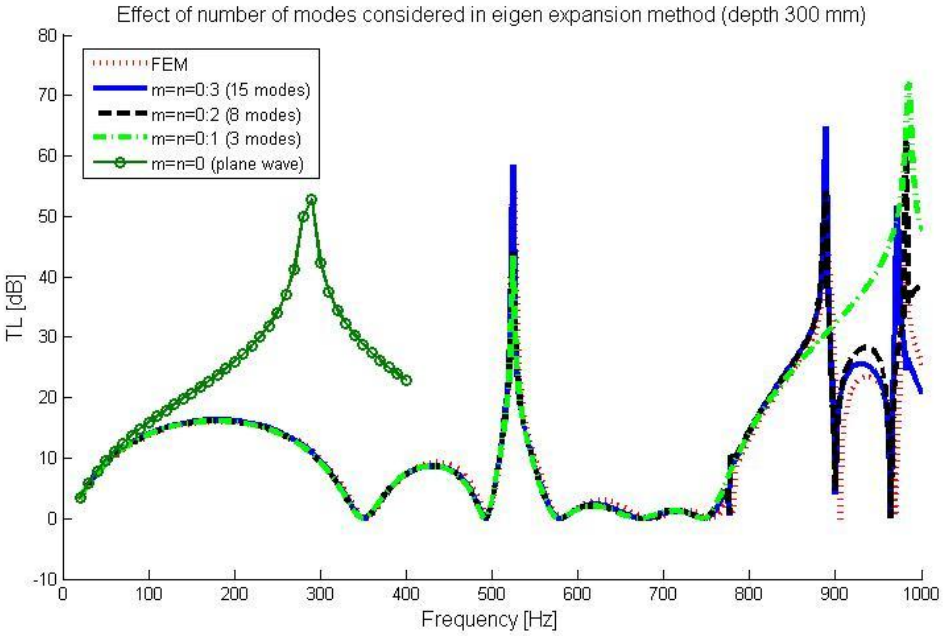

Figure 17

5.4 TL for a cylindrical chamber

In this part TL curves for a cylindrical chamber are compared in Figure 19. The geometry of the cylindrical chamber studied is shown in Figure 18 where geometry is symmetric around *x* and *y* and dimensions are:

$d = 0.206 \quad m$ $\qquad a_1 = a_2 = 0.056 \quad m$ $\qquad e_1 = e_2 = 0.043 \quad m$

$\theta_0 = 180°$ $\qquad depth = l = 0.207 \quad m$

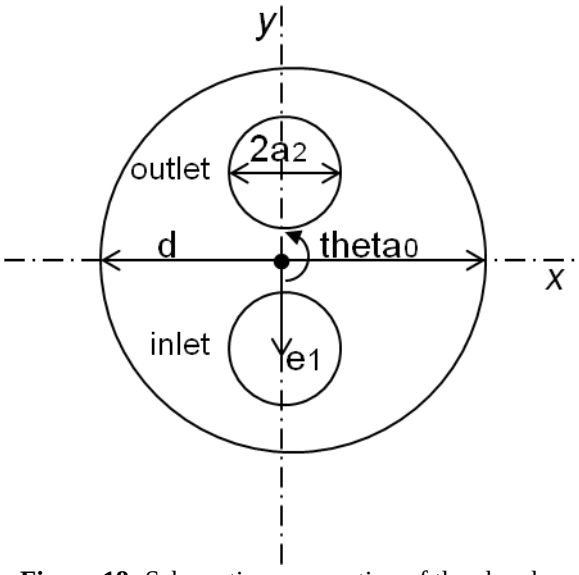

Figure 18: Schematic cross section of the chamber

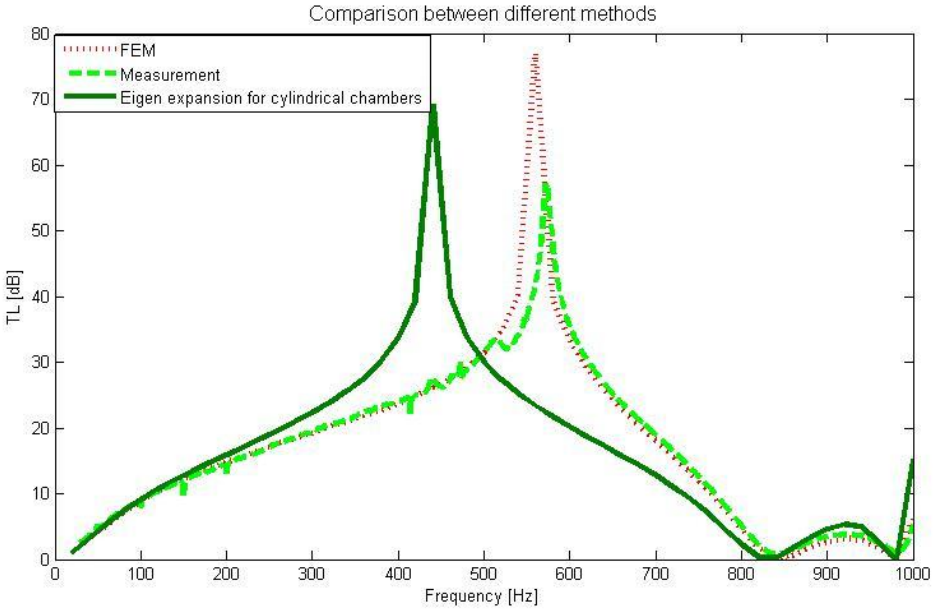

Figure 19

With respect to Figure 19 it can be said that the studied theory for cylindrical chambers is not correct and the reason for this was not found during this project.

6 Approximating chambers with round edges with rectangular ones

As discussed earlier in the introduction part, mufflers used in industry are not real rectangles. They are usually curved at the edges to increase the stiffness, see Figure 20. It is of interest for industry to know how this difference can alter the TL curve from a rectangular chamber. This problem can be solved by FEM, however this method would be expensive and time consuming. One method can be to approximate the chamber which has round edges with a rectangular one and then use the available theoretical models like the Green's function method to get TL curve. In this part we want to find out how to do this approximation.

To do this approximation, we can use the *Average Deviation (ADev)* which is defined in the following equation:

$$ADev = \frac{1}{N}\sum_{i=1}^{N}\left(\left|10^{\left(\frac{TL(f_i)_{TH}}{20}\right)} - 10^{\left(\frac{TL(f_i)_{FE}}{20}\right)}\right|\right) \qquad (6\text{-}1)$$

Where;

f: frequency [Hz]

TL_{TH} : Transmission loss calculated by theory [dB]

TL_{FE}: Transmission loss calculated by FE simulation for a chamber with rounded edges [dB]

N: Number of frequencies at which transmission matrix is evaluated

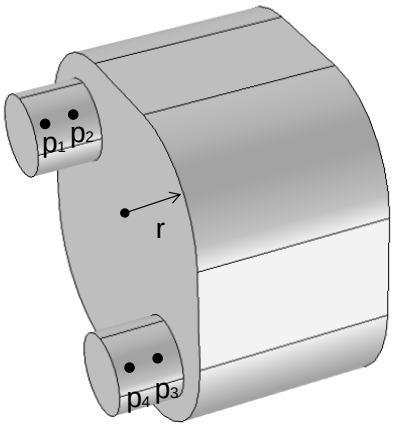

Figure 20. Example of a chamber with rounded edges and data extraction points.

To calculate *ADev*, first TL is calculated for an arbitrary chamber with round edges by FEM. Then a rectangular is modeled by theory (green's function method) with the same relative position and size of inlet and outlet but different width and depth. Range of selected width and depth are near to these properties of the chamber with round

edges itself. Finally all the theoretically calculated TLs are compared to the one from FEM by the use of *ADev*. Results would be like Table 1 Where the lowest value of *ADev* would determine the closest rectangular model to the one with round edges. To validate this methodology we simulate a chamber in COMSOL without fillet (rectangular chamber with square cross section) and choose width and length of the chamber to be 0.494 m and 0.3 m respectively. Expectation is to get the lowest value for *ADev* when geometries from simulation and theory are the same. Validation results are shown in Table 1 where given depths and widths are used in theoretical calculation.

		depth [m]					
		0,27	0,28	0,29	0,3	0,31	0,32
Width [m]	0,444	14,58	7,28	6,07	7,77	5,62	5,36
	0,454	6,65	6,96	18,55	5,91	7,86	5,26
	0,464	6,23	5,94	7,10	6,72	4,84	8,58
	0,474	7,48	6,14	5,22	7,55	4,23	4,60
	0,484	9,26	7,20	24,36	3,98	7,41	5,69
	0,494	6,05	6,07	4,28	2,91	5,13	7,74
	0,504	5,89	5,29	3,91	4,19	5,31	7,85
	0,514	49,53	4,99	132,40	4,67	5,52	6,03
	0,524	6,72	7,26	5,08	5,35	6,13	6,30

Table 1 ADev for different geometries under 1 kHz

As it was expected the lowest value is in the cross section of 0,3 and 0,494 (shaded box; Table 1); 2 more simulation of this kind is done which show this method works with a good approximation and can find the solution to our problem. So it can be said that one can find the best approximated model by finding minimum of *ADev* function. For calculation of Table 1 green's function method is used with $m=p=n=3$.

Next step is to use this methodology for different chambers with curved edges. However, in order to avoid too many tables just final results are shown in Table 2 and Table 4 for under cut on frequency of the first higher order mode and under 1 kHz respectively.

	Chamber with round edges (Real)				Best theoretical approximation			cross section ratio	volume ratio
chamber No.	width [m]	depth [m]	fillet radius [m]	cross section area [m^2]	width [m]	depth [m]	ADev	$C_A = \frac{A_{Real}}{A_{Approximated}}$	$\frac{V_{Real}}{V_{Approximated}}$
1	0.494	0,3	0.494/5	0.2357	0,474	0,31	0,06	1,05	1,02
2	0.494	0,3	0.494/4	0.231	0,464	0,32	0,06	1,07	1,01
3	0.494	0,3	0.494/3.5	0.2269	0,454	0,32	0,03	1,10	1,03
4	0.494	0,3	0.494/3	0.221	0,444	0,32	0,08	1,12	1,05
5	0,494	0,3	0,1800	0,2162	0,444	0,33	0,09	1,10	1,00
6	0,494	0,3	0,2000	0,2097	0,434	0,33	0,05	1,11	1,01
7	0,494	0,3	0,2200	0,2025	0,424	0,33	0,02	1,13	1,02
8	0,494	0,3	0,2400	0,1946	0,414	0,33	0,03	1,14	1,03
9	0,494	0,3	0,2470	0,1917	0,414	0,33	0,04	1,12	1,02
10	0,494	0,25	0,1235	0,2310	0,464	0,26	0,05	1,07	1,03
11	0,494	0,2	0,1235	0,2310	0,464	0,21	0,03	1,07	1,02
12	0,494	0,15	0,1235	0,2310	0,454	0,16	0,03	1,12	1,05

Table 2: Approximating the real geometry, considering frequencies under cut on of the first higher order mode.

To have a good approximation under cut on frequency, it seems volume should be kept constant. It should be kept constant by increasing the depth and decreasing width of the chamber, according to the results in Table 2. Figure 21 compares TL for a chamber with round edges and its approximated theoretical one under cut on frequency.

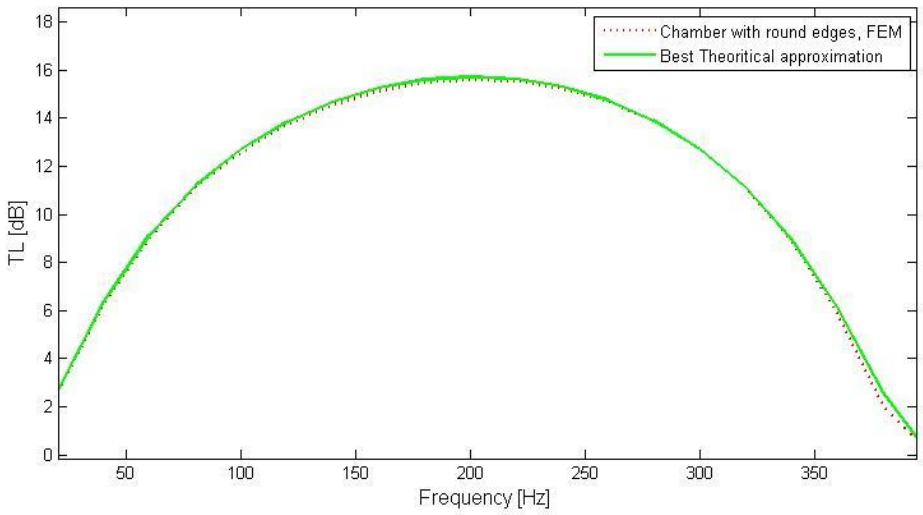

Figure 21: Results for chamber No. 6 in **Table 2**

However without having *FEM results* and *best theoretical approximation*, it seems hard to say how much width and depth of the chamber should be changed as *resizing factor* would be unknown. This factor can be defined as:

$$C_A = \frac{A_{real}}{A_{approximated}}$$ resizing factor

If C_A is known, depth and width of the rectangular chamber can be found by the following equations, see Figure 22:

$$d_r = C_A d \qquad w_r = \sqrt{\frac{A_{real}}{C_A}}$$

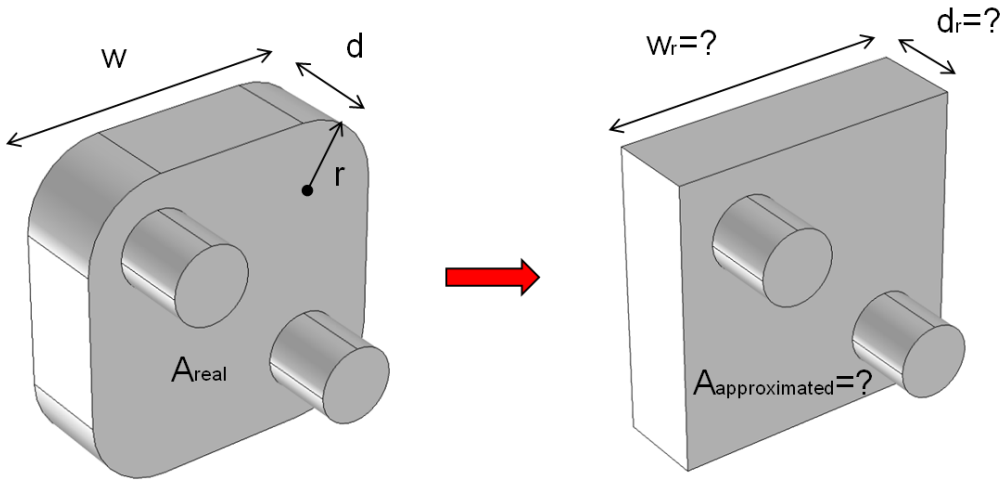

Figure 22: approximating a chamber with round edges with a rectangular one

C_A as stated earlier would be unknown without having *FEM results* and *best theoretical approximation*; however, it can be found from Table 2 that C_A varies just in a small range between 1.05 to 1.14. So to get a safe approximation, we can select some common resizing factors (like 1.07, 1.1, 1.12) to generate several rectangular chambers. Then these rectangular chambers will be used for Calculation of TL for a chamber with round edges. All these rectangular chambers would have the same volume as the volume of chamber with round edges while cross section area is reduced by inverse of C_A and depth is multiplied by C_A to keep the volume constant. Then approximated TL can be calculated as

$$TL(f)_{approximated} = 20\log\left(\frac{\sum_{1}^{k} 10^{\left(\frac{TL(f)_{TH,k}}{20}\right)}}{k}\right) \qquad (6\text{-}2)$$

Where *k* is the number of rectangular chambers used in the approximation.

To check if this method, which may be called *Average fitting*, is good enough or not, *ADev* defined in equation (5-1) can be edited in the following way

$$ADev_k = \frac{1}{N}\sum_{i=1}^{N}\left(\left|\frac{1}{k}\sum_{1}^{k} 10^{\left(\frac{TL(f_i)_{TH,k}}{20}\right)} - 10^{\left(\frac{TL(f_i)_{FE}}{20}\right)}\right|\right) \qquad (6\text{-}3)$$

and then results from Eq.(6-3), where k is selected to be 3 and factors for resizing the chamber are selected to be 1.07, 1.1, 1.12, are compared against results from Table 2 in the following table.

	Best theoretical model	Average fitting
chamber No.	$ADev$	$ADev_k$
1	0,06	0,22
2	0,06	0,17
3	0,03	0,14
4	0,08	0,10
5	0,09	0,08
6	0,05	0,07
7	0,02	0,08
8	0,03	0,09
9	0,04	0,09
10	0,05	0,11
11	0,03	0,08
12	0,03	0,05

Table 3: Checking acurracy of *Average fitting* method by comparing it to best theoritical models

Table 3 shows that *Average fitting* method can be used effectively to approximate TL of a chamber with round edges under cut on frequency with good accuracy and yet saves lots of time as there would be no need for *FEM* and calculation of *best theoretical approximation.* Figure 23 also shows that TL calculated by *Average fitting* method is compatible with exact results from FEM and best theoretical approximation.

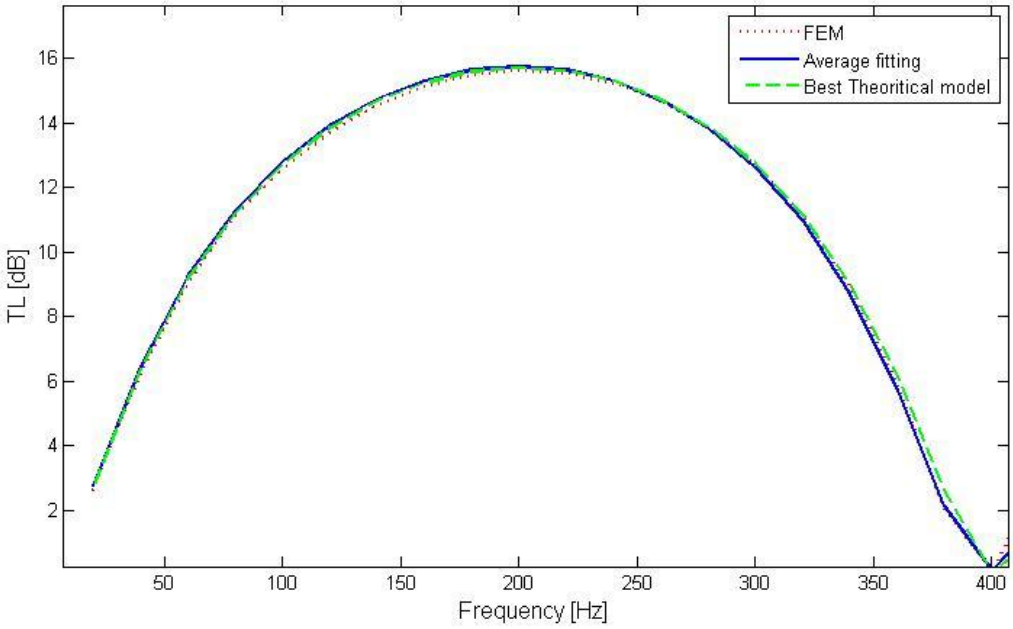

Figure 23: Results for chamber No.6 in **Table 2**

Table 4 Shows the same information as Table 2 except for the frequency range which is from 20 Hz to 1000 Hz. According to Table 4, it seems that it is not very straight forward to find a way for approximating the geometry of chambers with round edges while considering high frequency range as neither volume ratio nor cross section ratio are constant. Furthermore, ADev value is not small which means that even best matched theoretical models will introduce considerable error. As an example Results for chamber No. 6 is compared in Figure 24.

	Chamber with round edges (Real)				matched theoretical geometry			cross section ratio	volume ratio
chamber No.	width [m]	depth [m]	fillet radius [m]	cross section area [m^2]	width [m]	depth [m]	ADev	$C_A = \frac{A_{Real}}{A_{Approximated}}$	$\frac{V_{Real}}{V_{Approximated}}$
1	0,494	0,3	0,0988	0,2357	0,464	0,29	1,95	1,09	1,13
2	0,494	0,3	0,1235	0,2310	0,464	0,28	1,53	1,07	1,15
3	0,494	0,3	0,1411	0,2269	0,444	0,28	2	1,15	1,23
4	0,494	0,3	0,1647	0,2210	0,444	0,32	1,92	1,12	1,05
5	0,494	0,3	0,1800	0,2162	0,444	0,32	1,27	1,10	1,03
6	0,494	0,3	0,2000	0,2097	0,434	0,31	2,16	1,11	1,08
7	0,494	0,3	0,2200	0,2025	0,424	0,3	1,55	1,13	1,13
8	0,494	0,3	0,2400	0,1946	0,424	0,33	1,07	1,08	0,98
9	0,494	0,3	0,2470	0,1917	0,414	0,32	1,59	1,12	1,05
10	0,494	0,25	0,1235	0,2310	0,454	0,24	2,17	1,12	1,17
11	0,494	0,2	0,1235	0,2310	0,434	0,2	8,59	1,23	1,23
12	0,494	0,15	0,1235	0,2310	0,454	0,15	10,96	1,12	1,12

Table 4: Approximating the real geometry, considering frequencies under 1 kHz.

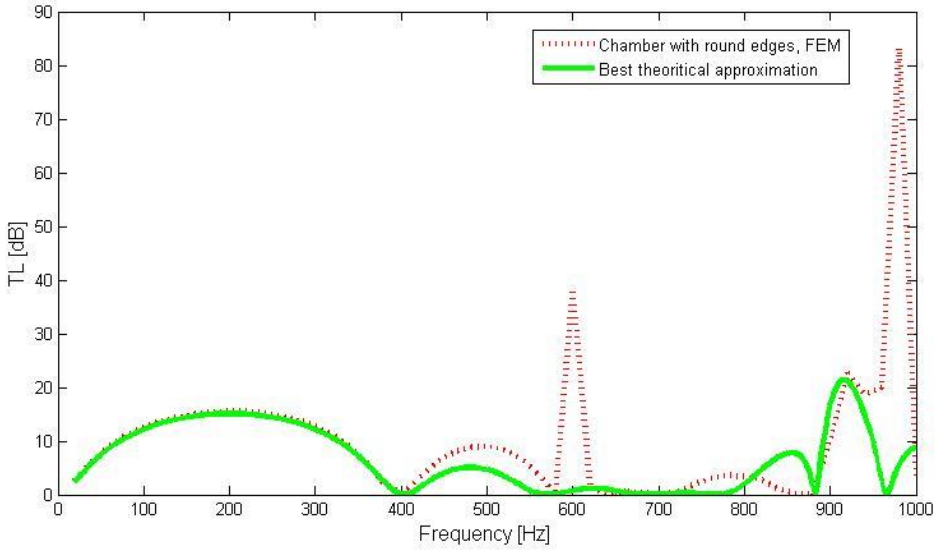

Figure 24: Results for chamber No. 6 in **Table 4**

7 Conclusions

During this study, two different theories for predicting TM and TL of rectangular chambers were studied [13, 16]. Results from these theories are in very good agreement with each other. Comparing TL results from theories with measurement and FEM, it was found that good results can be achieved once enough number of modes is considered in theoretical solutions; however, it was observed that there is a discrepancy between the TM results. This discrepancy may be solved by introducing acoustic length correction of duct extension into the chamber. Then it was shown that this discrepancy can mislead us even in calculation of insertion loss for a simple case silencer system.

As part of the study a theory for cylindrical chambers [1] was investigated and it was found that this theory is not exact enough

Afterwards, it was tried to approximate a chamber with round edges with a rectangular one by defining an objective function called *ADev* and trying to minimize it. Numerical calculations under cut on frequency of the first higher order mode showed that the best approximation is to keep the volume of the chamber with round edges constant. It should be kept constant by increasing the depth and decreasing width of the chamber. Finally, *Average fitting* was introduced as an accurate and quick method to predict TL of a chamber with round edges (under cut on frequency), based on the average acoustic behavior of several rectangular chambers.

8 References:

[1] J.-G. Ih AND B.-H. Lee, Theoretical prediction of the transmission loss of circular reversing chamber mufflers, *Journal of Sound and Vibration* (1987) 112(2) 261-272

[2] L. J. ERIKSSON 1982 *Silencers in Noise Control in Internal Combustion Engines*) editor D. E. Baxa). New York: John Wiley.

[3] H. E. HARTIG and C. E. S~,VANSON 1938 *Physical Review 54*" .626-618 ,Transverse" acoustic waves in rigid tubes.

[4] J. MILES 1944 *Journal of the Acoustical Society of America* .19-14 ,16 The reflection of sound due to a change in cross section of a circular tube.

[5] A. I. EL-SHARKAWY and A. H. NAYFEH 1978 *Journal of the Acoustical Society of America*,63 .674-667Effect of an expansion chamber on the propagation of sound in circular ducts.

[6] D. D. DAVIS, G. M. STOKES, D. MOORE and G. L. STEVENS 1954 *NACA Report*.1192 Theoretical and experimental investigation of mufflers with comments on engine-exhaust muffler design.

[7] P. TENGTRAIRAT and W. B. DIBOLL 1973 *Noise-CON* 73 *Proceedings* .217-212 Adjoint inlet-outlet quarter-wavelength mufflers.

[8] A. CRAGGS 1976 *Journal of Sound and Vibration* .392-377 ,48 A finite element method for damped acoustic systems: an application to evaluate the performance of reactive mufflers.

[9] T. SHUKU 1972 *Journal of the Acoustical Society of Japan* .12-5 ,28 Finite difference analysis of the acoustic field in irregular rooms.

[10] C.-I. J. YOUNG and M. J. CROCKER 1976 *Journal of the Acoustical Society of America 60,* .1118-1111Acoustical analysis, testing, and design of flow-reversing muffler chambers.

[11] M. N. Lindborg and M. Karlsson et al, Acoustic characterization of shallow flow reversal chambers, *SAE International*, 2011

[12] M. L. Munjal, a simple numerical method for three-dimensional analysis of simple expansion chamber mufflers of rectangular as well as circular cross-section with a stationary medium, *Journal of Sound and Vibration*, (1987) 116(1),71-88

[13] J.-G. Ih, The reactive attenuation of rectangular plenum chambers, *Journal of Sound and Vibration* (1992) 157(l), 93-122

[14] J.-G. Ih AND B.-H. Lee, Theoretical prediction of the transmission loss of circular reversing chamber mufflers, *Journal of Sound and Vibration* (1987) 112(2) 261-272

[15] Y. H. Kim, S. W. Kang, Green's solution of the acoustic wave equation for a circular expansion chamber with arbitrary locations of inlet, outlet port, and termination impedance, *Journal of the Acoustical Society of America* 94 (1)(1993)473–490.

[16] B. Venkatesham, Mayank Tiwari, M.L.Munjal, Transmission loss analysis of rectangular expansion chamber with arbitrary location of inlet/outlet by means of Green's functions, *Journal of Sound and Vibration* 323 (2009) 1032–1044

[17] M. FUKUDA, N. KOJIMA and T. IWAISH 1983 *Transactions of Japanese Society of Mechanical Engineers*)48 B), 1-9. A study on the mufflers with flow.

[18] L. Feng, *Acoustical Measurements*, KTH, ISSN 1651-7660, 4th print (2010)

[19] M.L.Munjal, Acoustics of Ducts and Mufflers, *Wiley*,NewYork,1987.

[20] P.M.Morse, K.U.Ingard, TheoreticalAcoustics, *McGraw-Hill*,NewYork,1968.

[21] Levine H. and Schwinger J., "On the radiation of sound from an un-flanged circular pipe", *Physical Review*, Vol. 73, pp. 383, 1948.]

[22] P. M. Morse 1981 *Vibration and Sound.* New York: Acoustical Society of America. See chapter 8.

[23] G. N. Watson 1966 *Theory of Bessel Functions.* London: Cambridge University Press, second edition. See chapters 11 and 18.

[24] http://www.sidlab.se/

[25] G.D.Callow and K.S.Peat 1988 *IMechE C19/88,* 39-46. Insertion loss of engine intake and exhaust silencers.